

How the antisymmetrization affects a cluster-cluster interaction: two-cluster systems

V. S. Vasilevsky^a, Yu. A. Lashko^{a,*}

^a*Bogolyubov Institute for Theoretical Physics,
Metrolohichna str., 14b, Kiev, 03143, Ukraine*

Abstract

We study effects of the antisymmetrization on the potential energy of two-cluster systems. The object of the investigation is the lightest nuclei of p -shell with a dominant α -cluster channel. For this aim we construct matrix elements of two-cluster potential energy between cluster oscillator functions with and without full antisymmetrization. Eigenvalues and eigenfunctions of the potential energy matrix are studied in detail. Eigenfunctions of the potential energy operator are presented in oscillator, coordinate and momentum spaces. We demonstrate that the Pauli principle affects more strongly the eigenfunctions than the eigenvalues of the matrix and leads to the formation of resonance and trapped states.

Keywords: cluster model, cluster-cluster interaction, potential energy matrix, oscillator basis, eigenvalues, eigenfunctions, separable representation

1. Introduction

The aim of this paper is to investigate effects of the Pauli principle on the potential energy of a two-cluster system. The object of the investigation is the lightest nuclei of p -shell with a dominant α -cluster channel. The method of the investigation is the algebraic version of the resonating group method [1, 2].

*Yu. A. Lashko

Email address: ylashko@gmail.com (Yu. A. Lashko)

The resonating group method (RGM) [3, 4, 5, 6, 7, 8] is a universal and efficient tool for studying properties of two-, three- and many-cluster systems. This method works perfectly for describing both compact many-cluster configurations and weakly bound states. It is also invaluable for studying different types of reactions and for predicting cross sections of the reactions which are, for example, important for the astrophysical applications. The main advantages of the method are that (i) it takes into account the internal structure of interacting clusters and (ii) correctly treats the Pauli principle. An important peculiarity of the RGM is that being applied to two- or three-cluster systems it reduces in a self-consistent way an A -body problem (where A is the number of nucleons) to a two- or three-body problem. The RGM strongly relies on the translationally invariant many-body shell model [9], [10], as this model supplies the wave functions describing the internal structure of clusters. Within the model, the internal antisymmetric wave functions of clusters are constructed from wave functions of three-dimensional harmonic oscillator. Such wave functions provide a reliable description of light atomic nuclei (the energy of the ground and excited states, the root-mean-square charge and mass radii and so on). It is then naturally to use oscillator wave functions also for describing the inter-cluster motion. At the beginning (see, for example, Refs. [11, 12] and book [13]) the oscillator basis was used to study bound states only by the diagonalization procedure. When the algebraic version of the resonating group method was formulated [1], [2], the oscillator basis have been used equally well for studying continuous spectrum states of many-channel and many-cluster systems.

The Pauli principle and a nucleon-nucleon interaction play the huge role in the rigorous realizations of the RGM such as the algebraic version of the RGM, the microscopic R matrix model [14] or the no-core shell model combined with the resonating group method [15, 16]. A nucleon-nucleon potential and the antisymmetrization determine the effective cluster-cluster interaction and thus strongly affects the dynamics of many-cluster systems.

It is well-known that correct treatment of the Pauli principle within microscopic models leads to bulky analytical expressions and time-consuming numerical calculations. To make calculations more simple, several alternative models for approximate treatment of the Pauli principle have been suggested. The most popular method is the orthogonality condition model (OCM) which was suggested by Saito [17, 5]. This method involves the folding approximation and orthogonality of the obtained wave functions to the Pauli forbidden states. The second method was suggested in Refs. [18, 19, 20] and was called

the pseudo-potential method. This method also employs the folding approximation for interacting clusters, but uses the separable pseudo-potential to eliminate the Pauli forbidden states.

It seems that everything is known about the Pauli principle. The Pauli principle has been investigated many times and from different points of view. A number of recipes have been formulated for constructing antisymmetric wave functions for different systems of identical fermions. Many results have been obtained revealing effects of the antisymmetrization on the structure of bound states and dynamics of reactions in many-particle systems. Huge efforts have been applied to study effects of the Pauli principle in two- and many-cluster systems. A number of publications is devoted to calculation of eigenvalues of the norm kernel and construction of the Pauli allowed states [21, 22, 23, 24, 25, 26, 27, 28, 29, 30, 31, 32]. Meanwhile, we are going to demonstrate that some interesting properties of the Pauli principle remained hidden and we are going to reveal some new intriguing features. We will demonstrate how the antisymmetrization affects a cluster-cluster potential energy.

As a tool for this study we employ the method suggested in Ref. [33]. As in Ref. [33], we will construct matrix of potential energy between oscillator functions and then analyze the eigenvalues and eigenfunctions of the matrix. The eigenfunctions will be analyzed in the oscillator, coordinate and momentum representations. Involving three different spaces allows us to get more complete picture on the nature and properties of the potential energy eigenfunctions. Besides, the method suggested in [33] allows one to reduce a nonlocal inter-cluster interaction to a local or separable form. It is than interesting to study what type of a local inter-cluster potential is provided by the diagonalization procedure. We employ three different nucleon-nucleon potentials which are often used in many-cluster calculations. These potentials will help us to demonstrate how eigenvalues and eigenfunctions of the potential energy operator depend on the shape of nucleon-nucleon potential.

It is important to notice that the total cluster-cluster interaction in a two-cluster system originates from the nucleon-nucleon interaction and also from the kinetic energy operator. The influence of the Pauli principle on the kinetic energy of relative motion of two clusters has been investigated in Refs. [29, 34, 32, 31]. It has been shown that the kinetic energy of a two-cluster system is not equivalent to the kinetic energy of a two-nucleon system due to the antisymmetrization effects. The kinetic energy operator of two-cluster relative motion modified by the Pauli principle generates an

effective interaction between clusters. The main properties of such interaction strongly correlate with the dependence of the eigenvalues of the norm kernel on the number of oscillator quanta. If the eigenvalues of the norm kernel of a two-cluster system approach unity from above with increasing the number of oscillator quanta, an effective attraction between cluster arises. At the same time, an effective inter-cluster repulsion appears in the case of the eigenvalues tending to unity from below. The radius of this interaction is determined by the range of oscillator quanta where the eigenvalues of the norm kernel differ from unity, while the intensity of the interaction depend on the rate of the eigenvalues approach unity. It was shown in Ref. [29] that the effective interaction generated by the kinetic energy operator of the relative motion between clusters can be strong enough to cause a resonance behavior of the phase shift of cluster-cluster scattering.

In the present paper we consider only the part of the cluster-cluster potential generated by the nucleon-nucleon potential with the focus on the Pauli effects.

The layout of the present paper is the following. In Sec. 2 we present a general framework of our investigations. Section 3 is devoted to numerical analysis of eigenvalues and eigenfunctions of potential energy operator for selected two-cluster systems. Concluding remarks and outlook are presented in Sec. 4.

2. Method

A wave function of A -nucleon systems for the partition $A = A_1 + A_2$ is

$$\Psi_{LM} = \hat{\mathcal{A}} \{ [\psi_1(A_1, s_1, b) \psi_2(A_2, s_2, b)]_S f_L(q) Y_{LM}(\hat{\mathbf{q}}) \}, \quad (1)$$

where $\psi_\nu(A_\nu, s_\nu, b)$ is a fully antisymmetric function, describing internal structure of the ν th cluster, $\hat{\mathcal{A}}$ is the antisymmetrization operator permuting nucleons belonging to different clusters and \mathbf{q} is the Jacobi vector determining distance between interacting clusters

$$\mathbf{q} = \sqrt{\frac{A_1 A_2}{A_1 + A_2}} \left[\frac{1}{A_1} \sum_{i \in A_1} \mathbf{r}_i - \frac{1}{A_2} \sum_{j \in A_2} \mathbf{r}_j \right]. \quad (2)$$

The wave functions $\psi_\nu(A_\nu, s_\nu, b)$ depend on spatial, spin and isospin coordinates of A_ν nucleons. They also depend on the oscillator length b , since they are the lowest functions of the translation-invariant oscillator shell model.

In Eq. (1) we assume that we deal with the s -clusters only, it means that $A_1, A_2 \leq 4$ and the intrinsic orbital momentum of each cluster equals zero. The total spin S is a vector sum of the individual spins of clusters s_1 and s_2 .

If we omit the antisymmetrization operator in (1), we have got the so-called folding approximation

$$\Psi_{LM}^{(F)} = [\psi_1(A_1, s_1, b) \psi_2(A_2, s_2, b)]_S f_L^{(F)}(q) Y_{LM}(\hat{\mathbf{q}}). \quad (3)$$

This approximate form is valid when the distance between clusters is large and effects of the Pauli principle are negligibly small. In what follows we will discuss in detail how large is this distance.

The function $f_L^{(F)}(q)$ is a solution of the two-body Schrödinger equation

$$\left\{ \hat{T}_q + V^{(F)}(q) + E^{(th)} - E \right\} f_L^{(F)}(q) = 0, \quad (4)$$

where

$$\hat{T}_q = -\frac{\hbar^2}{2m} \left[\frac{d^2}{dq^2} + \frac{2}{q} \frac{d}{dq} - \frac{L(L+1)}{q^2} \right]$$

is the kinetic energy operator and $V^{(F)}(q)$ is a folding or direct potential which is defined as

$$\begin{aligned} V^{(F)}(q) &= \int d\tau_1 d\tau_2 |\psi_1(A_1)|^2 |\psi_2(A_2)|^2 \sum_{i \in A_1} \sum_{j \in A_2} \hat{V}(\mathbf{r}_{ij}) \\ &= \int d\mathbf{r}_1 d\mathbf{r}_2 \rho_1(\mathbf{r}_1) \rho_2(\mathbf{r}_2) \hat{V} \left(\mathbf{r}_1 - \mathbf{r}_2 + \sqrt{\frac{A_1 + A_2}{A_1 A_2}} \mathbf{q} \right). \end{aligned} \quad (5)$$

Here $\rho_1(\mathbf{r}_1)$ ($\rho_2(\mathbf{r}_2)$) is a single particle local density of the first (second) cluster, and \mathbf{r}_1 (\mathbf{r}_2) is a coordinate of a nucleon with respect to the center of mass of the corresponding cluster. For s -nuclei, which are described by the lowest many-body shell model functions, the folding potential of the Coulomb and NN forces, having Gaussian coordinate form, has a simple analytical form. Folding potentials have been very often used in numerous calculations of elastic and inelastic processes.

The exact two-cluster potential is a nonlocal operator

$$V_L^{(E)}(\tilde{q}, q) = \left\langle \hat{\mathcal{P}}_L(\tilde{q}) \left| \hat{V} \right| \hat{\mathcal{P}}_L(q) \right\rangle, \quad (6)$$

where

$$\hat{V} = \sum_{i < j} \hat{V}(\mathbf{r}_{ij}) \quad (7)$$

is the total potential energy of the system and

$$\hat{\mathcal{P}}_L(q) = \hat{\mathcal{A}}\{[\psi_1(A_1, s_1, b) \psi_2(A_2, s_2, b)]_S \delta(r - q) Y_{LM}(\hat{\mathbf{r}})\}. \quad (8)$$

Operator $\hat{\mathcal{P}}_L(q)$ reduces the A -body space to an effective two-body space.

It is well-known that the inter-cluster wave function $f_L(q)$ is a solution to the integro-differential equation. This equation can be transformed to a simpler form and than can be much easily solved, when the function $f_L(q)$ is expanded into a complete set of the oscillator functions

$$f_L(q) = \sum_{n=0}^{\infty} C_{nL} \Phi_{nL}(q, b), \quad (9)$$

where C_{nL} is the expansion coefficient and $\Phi_{nL}(q, b)$ is the radial part of an oscillator wave function, n is the number of radial quanta. Oscillator length b for the oscillator function is selected the same as for many-particle oscillator functions describing the internal structure of interacting clusters.

Note that function $f_L(p)$ in momentum space has the same expansion coefficients

$$f_L(p) = \sum_{n=0}^{\infty} C_{nL} \Phi_{nL}(p, b). \quad (10)$$

Oscillator functions in coordinate and momentum space are very similar

$$\begin{Bmatrix} \Phi_{nL}(q, b) \\ \Phi_{nL}(p, b) \end{Bmatrix} = N_{nL} \rho^L e^{-\frac{1}{2}\rho^2} L_n^{L+1/2}(\rho^2) \cdot \begin{Bmatrix} (-1)^n b^{-3/2} \\ b^{3/2} \end{Bmatrix}, \quad \begin{matrix} \rho = r/b, \\ \rho = pb, \end{matrix} \quad (11)$$

where normalization coefficient N_{nL} is defined as

$$N_{nL} = \sqrt{\frac{2 n!}{\Gamma(n + L + 3/2)}}.$$

These functions are orthonormal and obey the completeness relation.

One can find in [35],[36] all necessary details of calculating matrix elements of potential energy for nuclei under consideration.

We have to construct the antisymmetric cluster basis functions

$$|nL\rangle_C = \hat{\mathcal{A}}\{[\psi_1(A_1, s_1, b) \psi_2(A_2, s_2, b)]_S \Phi_{nL}(q, b) Y_{LM}(\hat{\mathbf{q}})\} \quad (12)$$

and the folding cluster basis functions

$$|nL\rangle_F = [\psi_1(A_1, s_1, b) \psi_2(A_2, s_2, b)]_S \Phi_{nL}(q, b) Y_{LM}(\hat{\mathbf{q}}). \quad (13)$$

Both sets of functions are complete and orthogonal. In what follows we will omit labels s_1 , s_2 and b . Folding functions $|nL\rangle_F$ are orthonormal, while antisymmetric cluster basis functions $|nL\rangle_C$ are not normalized to unity:

$$\langle nL | \tilde{n}L \rangle_C = \Lambda_{nL} \delta_{n, \tilde{n}},$$

where Λ_{nL} are the well-known eigenvalues of the norm kernel.

By using the cluster basis functions $\{|nL\rangle_C\}$, one obtains the two-cluster Schrödinger equation in the form

$$\sum_{m=0} \left\{ \langle nL | \hat{H} | mL \rangle_C - E \Lambda_{nL} \delta_{n,m} \right\} C_{mL} = 0, \quad (14)$$

where $\langle nL | \hat{H} | mL \rangle_C$ is a matrix element of a microscopic two-cluster Hamiltonian. If we introduce an orthonormal set of the antisymmetric cluster functions

$$|nL\rangle_E = \frac{1}{\sqrt{\Lambda_{nL}}} |nL\rangle_C = \frac{1}{\sqrt{\Lambda_{nL}}} \hat{\mathcal{A}} \{ \psi_1(A_1) \psi_2(A_2) \Phi_{nL}(q, b) Y_{LM}(\hat{\mathbf{q}}) \}, \quad (15)$$

we will get the Schrödinger equation (14) in the form

$$\sum_{m=0}^{\infty} \left\{ \langle nL | \hat{H} | mL \rangle_E - E \delta_{n,m} \right\} C_{mL} = 0, \quad (16)$$

which is typical for an orthonormal basis of functions.

In what follows, it is assumed the energy of two-cluster systems is determined with respect to the two-cluster threshold. Hence the internal kinetic and potential energy of interacting clusters is subtracted from the Hamiltonian \hat{H} of a two-cluster system. Therefore, both exact $V_L^{(E)}(q, q)$ and folding $V^{(F)}(q)$ potential energies tend to zero as the coordinate q approaches infinity and thus both of them represent the potential energy of cluster-cluster interaction. Moreover, the exact $V_L^{(E)}(\tilde{q}, q)$ potential energy for large values of \tilde{q} and q becomes local and coincides with the folding potential $V^{(F)}(q)$.

The first effect of the Pauli principle on two-cluster systems is connected with appearance of the Pauli forbidden states. The Pauli forbidden states

are those cluster basis functions (12) which are annihilated by the antisymmetrization operator. The eigenvalues of the norm kernel corresponding to the Pauli forbidden states are equal to zero. Thus the Pauli principle forbids such basis functions [27], [37], [17], [5]. The Pauli forbidden states are the cluster basis functions with the lowest values of the quantum number n . The number of the forbidden states depends on the clusterization and the total orbital momentum L of a compound system. For example, for the 0^+ state in ${}^8\text{Be} = \alpha + \alpha$, the Pauli principle annihilates two cluster functions $|n=0, L=0\rangle_C$ and $|n=1, L=0\rangle_C$, and thus two first columns and rows of the potential energy matrix equal zero.

The second effect of the Pauli principle can be seen in Eq. (15). It renormalizes the two-cluster oscillator functions and, consequently, matrix elements of the potential energy operator as

$$\langle nL | \hat{V} | mL \rangle_E = \frac{1}{\sqrt{\Lambda_{nL}}} \langle nL | \hat{V} | mL \rangle_C \frac{1}{\sqrt{\Lambda_{mL}}}. \quad (17)$$

It is obvious that if $\Lambda_{nL} > 1$, the matrix elements $\langle nL | \hat{V} | mL \rangle_E$ are decreased with respect to the matrix elements $\langle nL | \hat{V} | mL \rangle_C$. If $\Lambda_{nL} < 1$, the matrix elements $\langle nL | \hat{V} | mL \rangle_E$ are increased.

We will use the set of functions (15) to calculate matrix elements of potential energy with the exact treatment of the Pauli principle. It is interesting to analyze how the eigenvalues of the norm kernel change potential energy of two-cluster system.

2.1. Matrix elements

Having constructed matrix of potential energy $\| \langle nL | \hat{V} | mL \rangle \|$ of dimension $N \times N$, we can calculate eigenvalues λ_α ($\alpha=1, 2, \dots, N$) and corresponding eigenfunctions $\{U_n^\alpha\}$ of the matrix. Actually, we use the decomposition of the matrix into diagonal matrix $\|\lambda\|$ and orthogonal one $\|U\|$:

$$\| \langle nL | \hat{V} | mL \rangle \| = \|U^{-1}\| \|\lambda\| \|U\| \quad (18)$$

or

$$\langle nL | \hat{V} | mL \rangle = \sum_{\alpha=1}^N U_n^\alpha \lambda_\alpha U_m^\alpha, \quad (19)$$

where

$$\|\lambda\| = \left\| \begin{array}{cccc} \lambda_1 & & & \\ & \lambda_2 & & \\ & & \ddots & \\ & & & \lambda_N \end{array} \right\|. \quad (20)$$

The orthogonal matrix $\|U\|$ generates a new set of inter-cluster functions ϕ_α and two-cluster wave functions Ψ_α

$$\phi_\alpha(q, b) = \sum_n U_n^\alpha \Phi_{nL}(q, b) \quad (21)$$

$$\Psi_\alpha = \hat{\mathcal{A}}\{\psi_1(A_1) \psi_2(A_2) \phi_\alpha(q, b) Y_{LM}(\hat{\mathbf{q}})\}. \quad (22)$$

The functions $\phi_\alpha(q, b)$ and eigenvalues λ_α enable us to construct inter-cluster nonlocal potential

$$\hat{V}_N(q, \tilde{q}) = \sum_{\alpha=1}^N \phi_\alpha(q, b) \lambda_\alpha \phi_\alpha(\tilde{q}, b). \quad (23)$$

This is an approximate form of the inter-cluster potential. One can get an exact form of the potential as a limit of the expression

$$\hat{V}(q, \tilde{q}) = \lim_{N \rightarrow \infty} \hat{V}_N(q, \tilde{q}).$$

Note, that for the folding (direct) potential, we have got

$$\hat{V}(q) \delta(q - \tilde{q}) = \lim_{N \rightarrow \infty} \hat{V}_N(q, \tilde{q}).$$

In what follows we are going to study properties of the eigenvalues and eigenfunctions of the potential energy operator in the oscillator representation $\{U_n^\alpha\}$, coordinate $\phi_\alpha(q, b)$ and momentum $\phi_\alpha(p, b)$ spaces.

Note that the formula (23) is one of the numerous methods of the separable representation in quantum mechanics (see review and books about the separable representations in [38], [39], [40]). For a two-body case, the eigenfunctions $\phi_\alpha(q, b)$ or $\phi_\alpha(p, b)$ would immediately define a wave function and t-matrix, as it was demonstrated in Ref. [33]. However, in two-cluster systems the antisymmetrization is known to affect the kinetic energy and norm kernel and thus the kinetic energy and norm kernel participate in creating the effective cluster-cluster interaction as well.

When $L \geq A - 4$, eigenfunctions of exact and folding approximation are very close to each other. However, for small values of n one can see the trace of the antisymmetrization operator.

Table 1: Oscillator length b in fm for different nuclei and different potentials.

Nucleus	VP	MHNP	MP
$^5\text{He}, ^5\text{Li}$	1.38	1.32	1.28
^6Li	1.46	1.36	1.31
$^7\text{Li}, ^7\text{Be}$	1.44	1.36	1.35
^8Be	1.38	1.32	1.28

3. Results

We employ three nucleon-nucleon potentials which have been often used in different realizations of the cluster model. In our calculations we involve the Volkov N2 (VP) [41], modified Hasegawa-Nagata (MHNP) [42, 43] and Minnesota (MP) [44] potentials. Coulomb forces are also involved in calculations and treated exactly. For the sake of simplicity we neglect the spin-orbit forces, thus the total spin S and the total orbital momentum L are good quantum numbers. Oscillator length b is selected to optimize energy of the lowest decay threshold for each nucleus and for each NN potential. The optimal values of b are shown in Tab. 1.

Figures 1 and 2 demonstrate the main differences between the MHNP, MP and VP potentials. In these figures we display only the even components V_{31} and V_{13} of all three NN potentials. It is known, that the even components are stronger than the odd components. Indeed, the V_{31} component provides a bound state in a deuteron and the V_{13} component generates a virtual state in the neutron-neutron system. One can see that the MHNP has the largest repulsive core at small distances, the MP has a soft core and the VP has a negligibly small core. Fig. 2 provides detailed view of these potentials. We observe from this figure that the larger is the core in the potential, the deeper is the attractive part of the potential.

Nuclei under consideration together with their corresponding two-cluster configurations are listed in Table 2. One can see that all nuclei are represented by the lowest and thus dominant two-cluster channel.

In what follows, we will consider matrix elements of potential energy operator between the Pauli allowed states and will neglect the Pauli forbidden states. This will lead to somewhat different numeration of basis functions (12) and matrix elements (17). The quantum number n we substitute with a new quantum number

$$n \rightarrow n_0 + n, \quad (24)$$

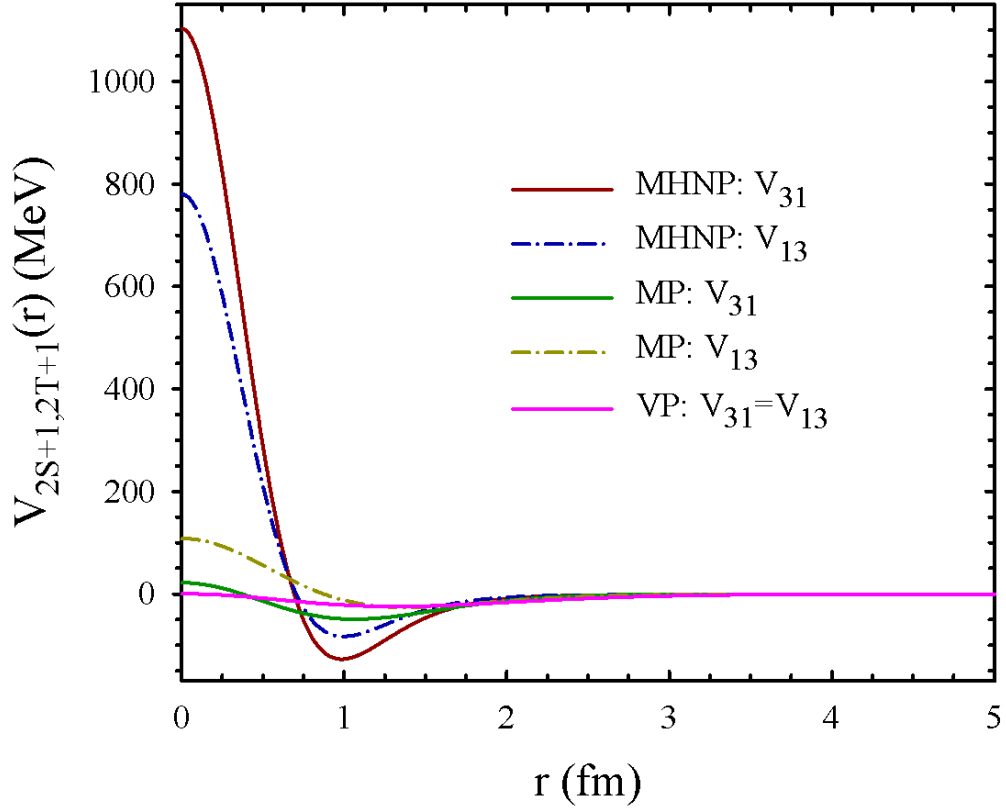


Figure 1: Even components of the MHNP, MP and VP potentials as a function of distance between nucleons.

Table 2: List of nuclei and two-cluster configurations

Nucleus	Configuration
${}^5\text{He}$	${}^4\text{He}+n$
${}^5\text{Li}$	${}^4\text{He}+p$
${}^6\text{Li}$	${}^4\text{He}+d$
${}^7\text{Li}$	${}^4\text{He}+{}^3\text{H}$
${}^7\text{Be}$	${}^4\text{He}+{}^3\text{He}$
${}^8\text{Be}$	${}^4\text{He}+{}^4\text{He}$

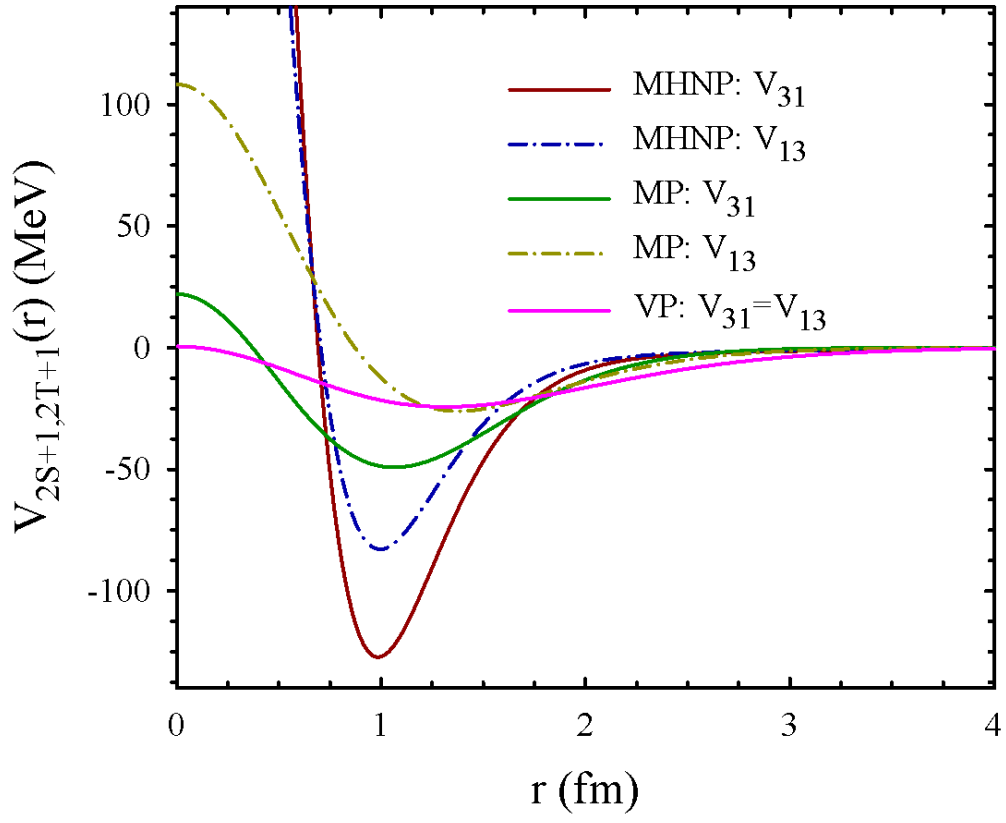


Figure 2: An attractive part of the even components of the MHNP, MP and VP.

where n ($n = 0, 1, \dots$) numerates the Pauli allowed states, and n_0 is the number of the Pauli forbidden states

$$n_0 = \begin{cases} \max((A - 4 - L)/2, 0) & \pi = (-)^A = (-)^L \\ \max((A - 3 - L)/2, 0) & \pi = (-)^{A+1} = (-)^L \end{cases} \quad (25)$$

The first row of this equation is valid for normal parity states, while the second row is valid for abnormal parity states. It is easy to deduce from Eq. (25) that there are no Pauli forbidden states for the total angular momentum $L \geq (A - 4)$ (the normal parity states) or for $L \geq (A - 3)$ (the abnormal parity states). In the nuclei under consideration the number of the Pauli forbidden states is very small. For example, there is only one Pauli forbidden state in the abnormal parity 0^+ state of ^5He and ^5Li , and there are two Pauli forbidden states in the 0^+ states of ^7Li , ^7Be and ^8Be .

3.1. Eigenvalues of the norm kernel.

First, we calculate eigenvalues of the norm kernel. They are displayed in Fig. 3 as a function of N_{osc} , the number of oscillator quanta

$$N_{osc} = 2n + L.$$

The eigenvalues are displayed for normal parity (triangles up) and for abnormal parity (triangles down) states. One can see that the antisymmetrization affects only few cluster basis states with $N_{osc} \leq 25$. We can estimate the "range" of the Pauli principle by using correspondence between oscillator and coordinate spaces:

$$R_P \approx b \sqrt{\frac{A_1 + A_2}{A_1 A_2}} \sqrt{2N_{osc} + 3} \approx 10 \text{ fm}.$$

Fig. 3 also demonstrates that for nuclei ^5He , ^5Li , ^6Li , ^7Li , ^7Be the eigenvalues of the norm operator $\Lambda_{nL} > 1$ for the normal parity states and $\Lambda_{nL} < 1$ for the abnormal parity states.

In Fig 4 we display folding potentials for ^5He , ^5Li , ^6Li , ^7Li , ^7Be , and ^8Be created by the MHNP nucleon-nucleon potential and the Coulomb interaction between protons. It is worthwhile noticing that despite of the huge core in this nucleon-nucleon potential, there is no such a core in the cluster-cluster folding potential. Only in ^5He and ^5Li nuclei we can see a small repulsive core at small inter-cluster distances. The lower part of Fig. 4 demonstrates the shape and height of a barrier created by the Coulomb interaction.

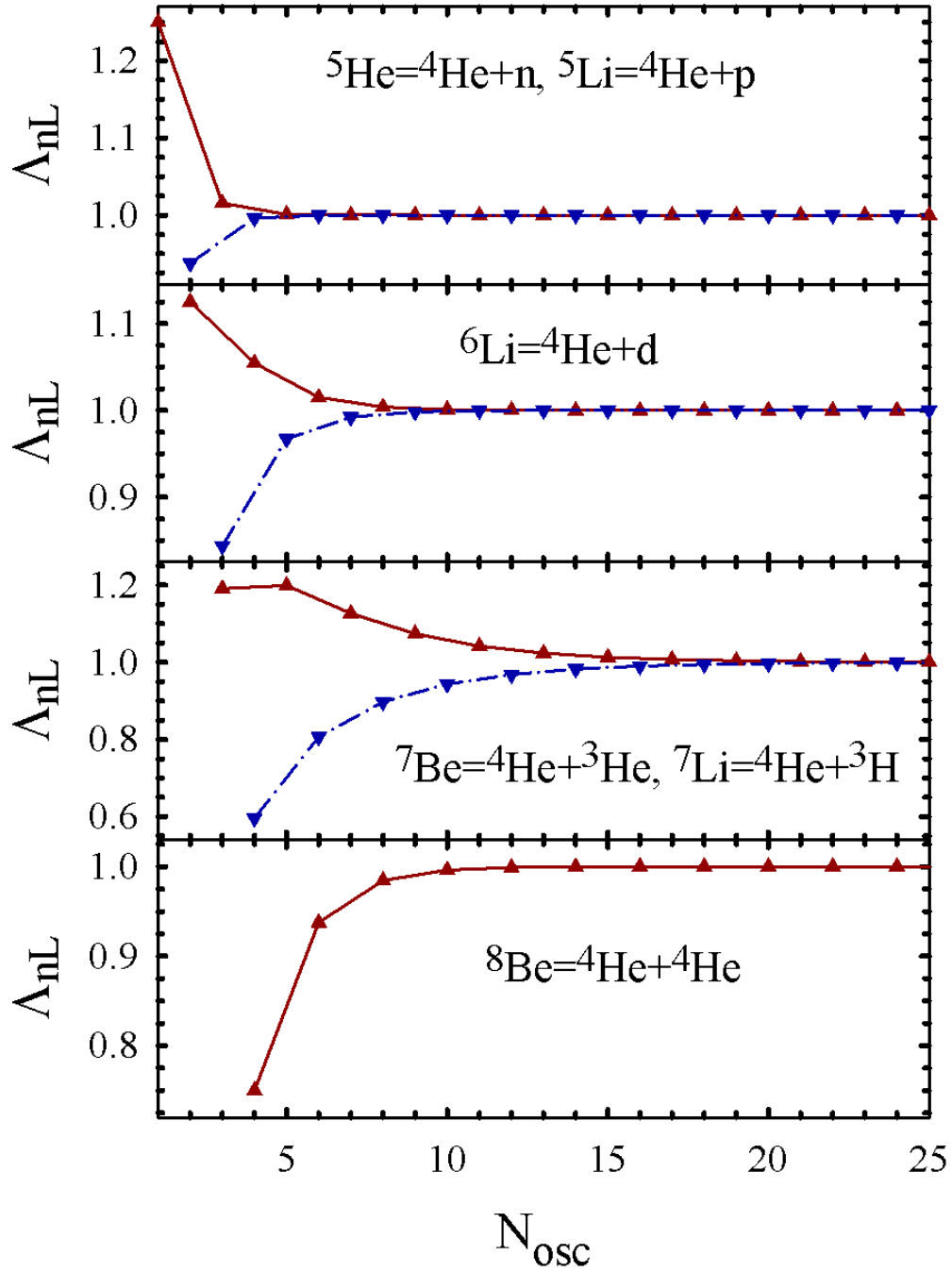


Figure 3: Eigenvalues of the norm kernel for the lightest p -shell nuclei. Triangles up represent the eigenvalues for the normal parity states, and triangles down demonstrate them for the abnormal parity states.

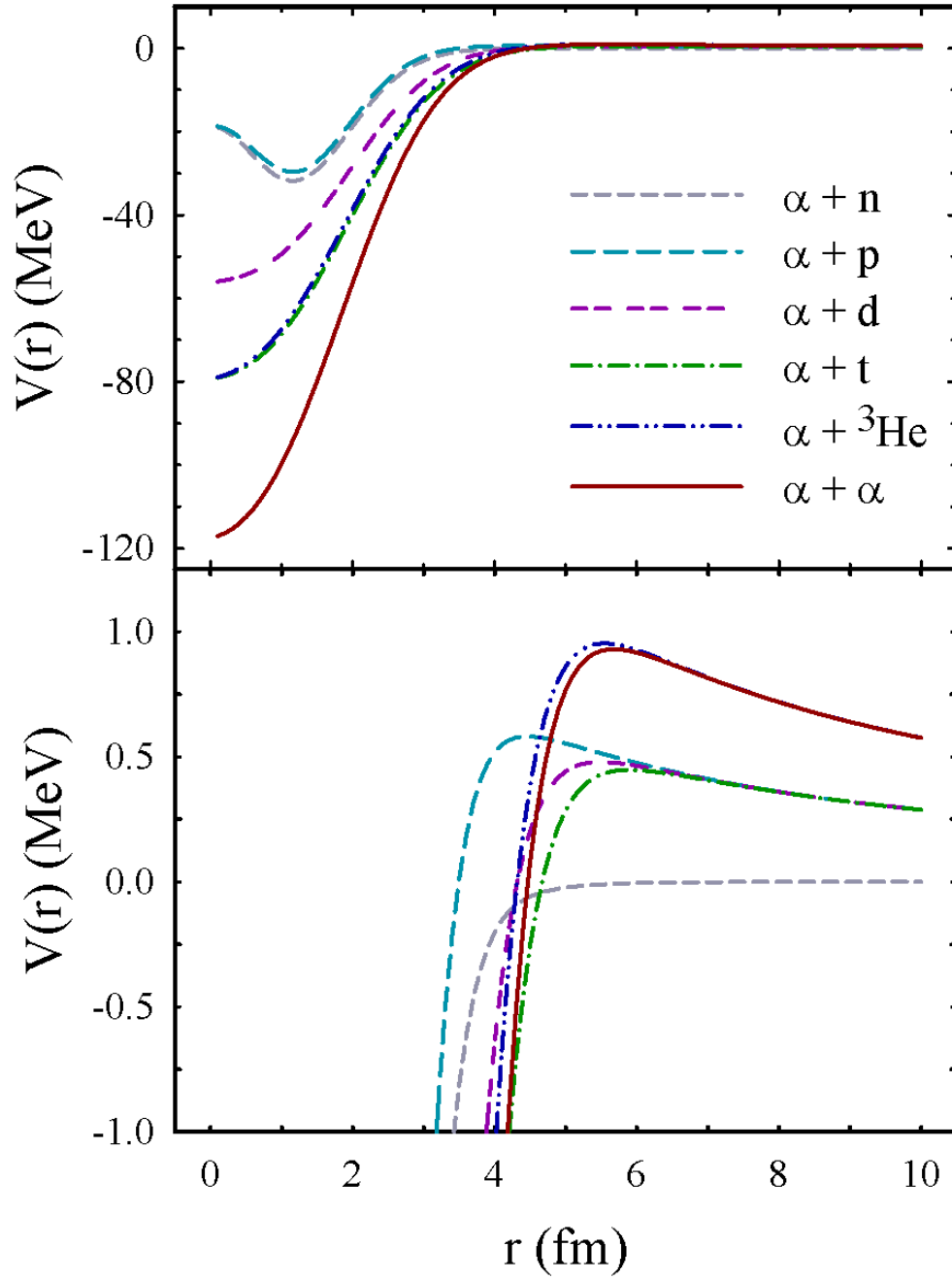


Figure 4: Folding potential generated by the MHN potential as a function of the distance between interacting clusters for the lightest p -shell nuclei.

In Fig. 5 we display the folding potentials created by the VP. As we pointed out above, this nucleon-nucleon potential has no repulsive core. However, it creates a small repulsive core between α -particle and a neutron in ${}^5\text{He}$. Different NN potentials create approximately the same shape of the cluster-cluster folding potential. The main difference between the folding potentials, generated by different NN potentials, is depths and width of the potential well.

3.2. Matrix of potential energy.

In Figs. 6 and 7 we demonstrate general features of matrix of the exact and folding potentials, respectively. These matrices are calculated for the 0^+ state in ${}^8\text{Be}$ with the MHNP potential and look very similar, except the region of very small number of quanta. Matrix elements of the exact and folding potentials have the same structure. As evident from Figs. 6 and 7, nonzero matrix elements are concentrated around the main diagonal of the potential matrix. Along this diagonal the matrix elements are slowly decreasing. This is a general behavior of matrix elements of the potential energy operator for all nuclei under considerations, for all values of the total orbital momentum L and for all nucleon-nucleon potentials involved in calculations.

3.3. Eigenvalues

In Fig 8 we display eigenvalues of the potential energy matrix for $L^\pi = 1^-$ state of ${}^7\text{Li}$, calculated for the MHNP potential with 300 basis functions. One can see that the eigenvalues of the potential energy matrix, calculated with antisymmetrization (in what follows we will mark it with the letter E), are very close to the ones determined in the folding approximation (we mark them with the letter F). The lowest eigenvalues almost coincide, indicating that both potentials have the same depth. One can also see that the exact potential is less attractive in the range $5 \leq \alpha \leq 30$. Besides, the eigenvalues of the exact potential reveal some irregularities, which are absent for the folding potential eigenvalues. Below it will be shown that they correspond to resonance states generated by the Pauli exclusion principle. For $\alpha > 50$ the exact potential is very close to the folding potential. Similar behavior of eigenvalues is observed for all lightest nuclei of the p -shell and for all NN potentials involved in our calculations.

In Fig. 9 we show eigenvalues λ_α for all lightest p -shell nuclei obtained with the MHNP. The eigenvalues are displayed for the "ground states" of

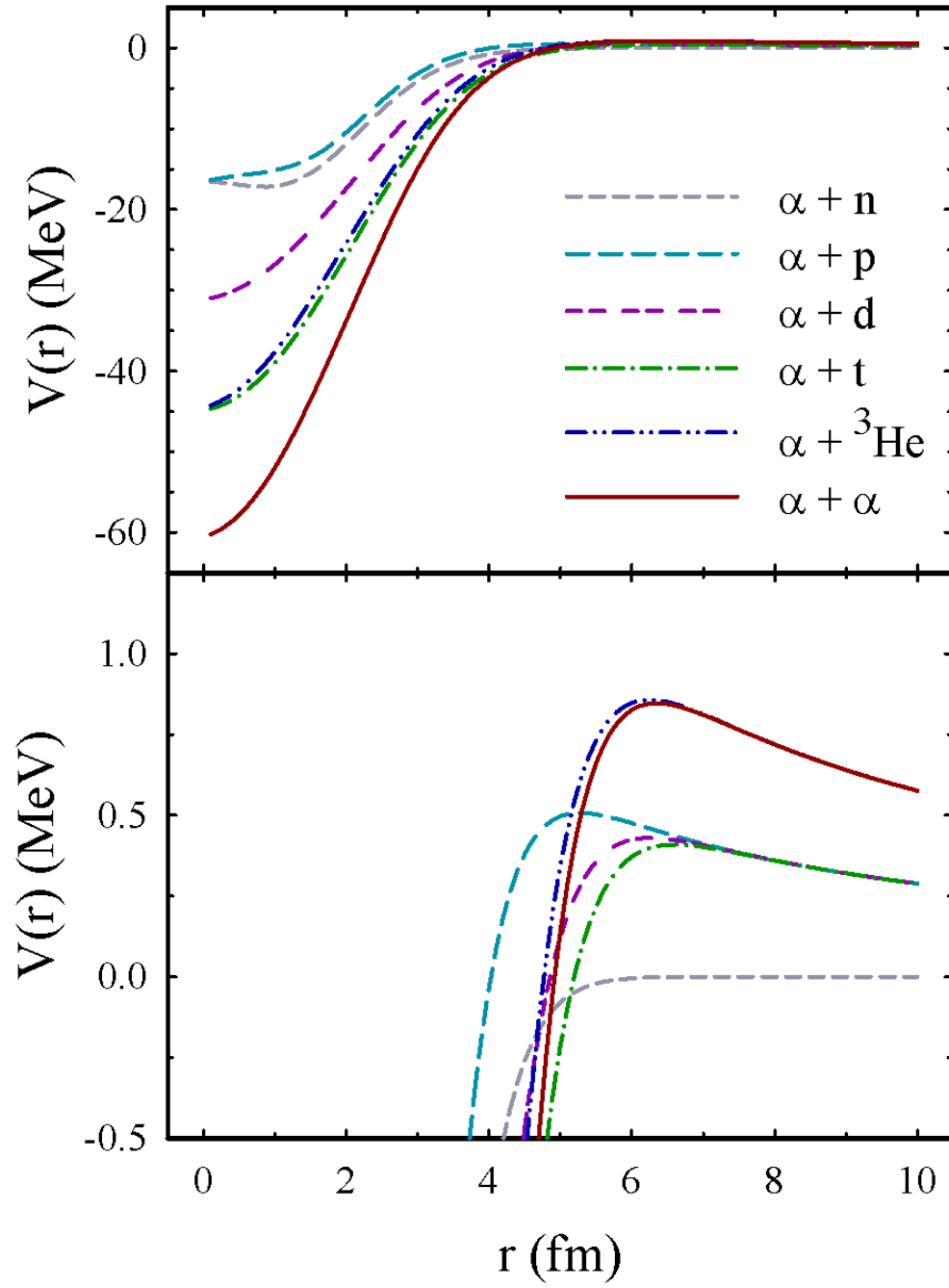


Figure 5: Folding potentials generated by the VP.

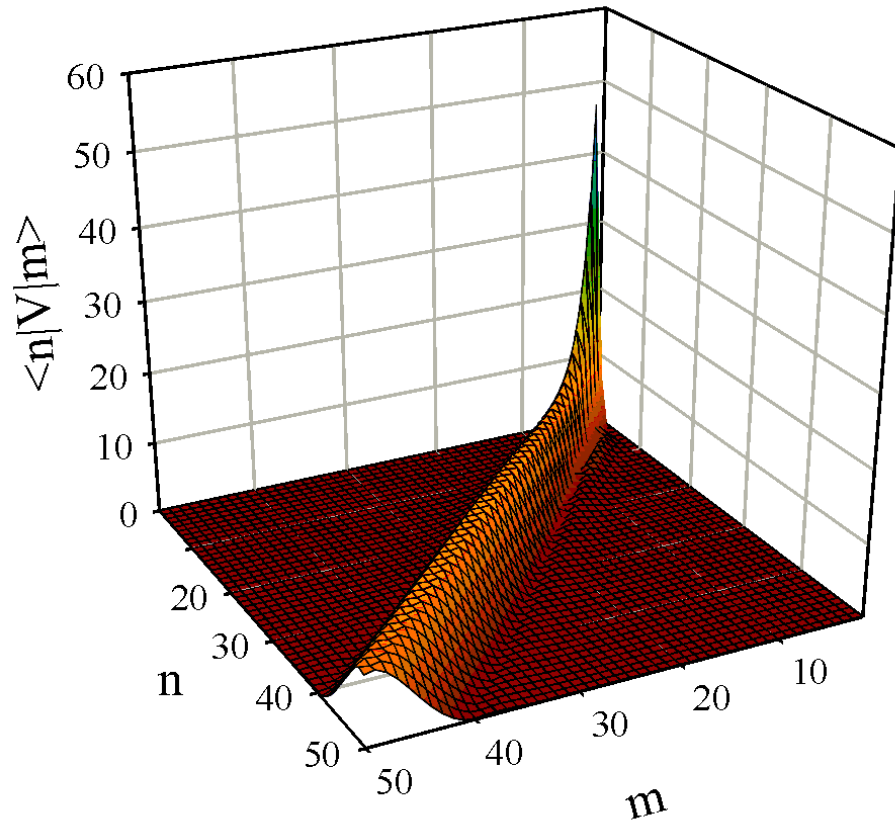


Figure 6: Matrix elements of the exact potential energy operator calculated for the 0^+ state of ^8Be with the MHNP.

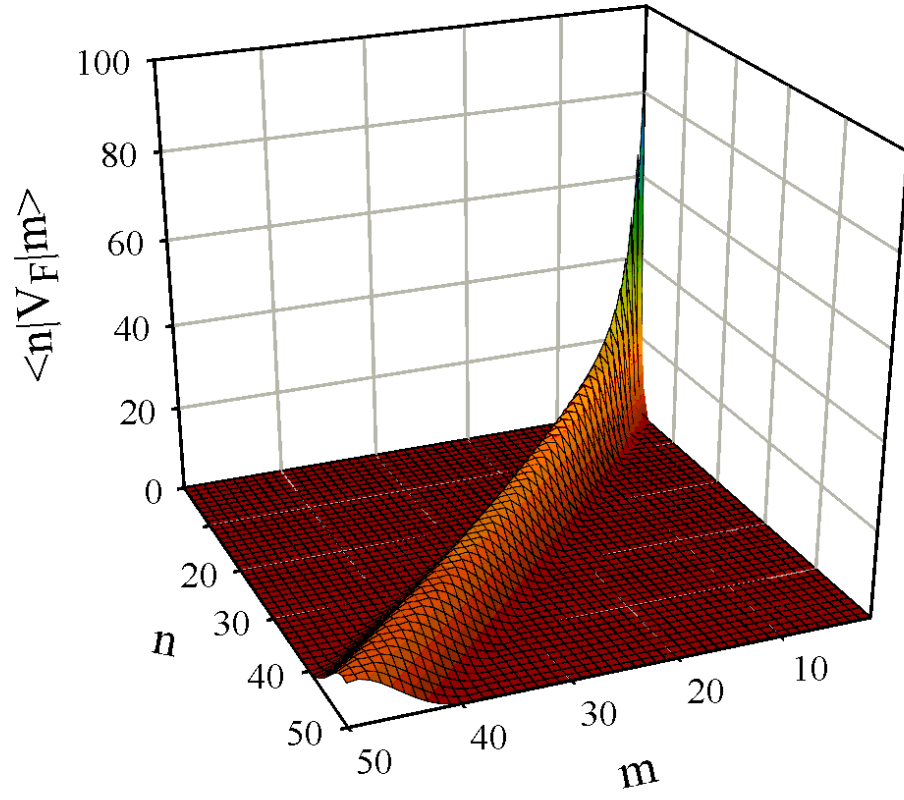


Figure 7: Matrix elements of the folding potential energy operator calculated for the 0^+ state of ^8Be with the MHNP.

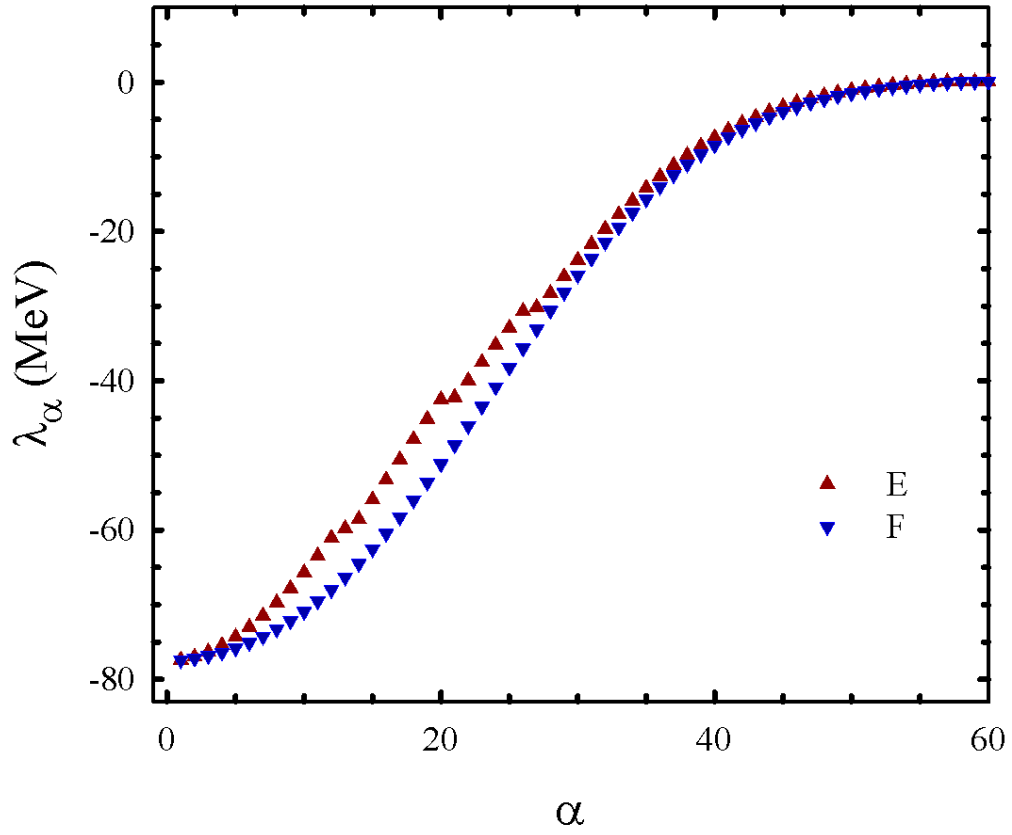


Figure 8: Eigenvalues of the exact (E) and folding (F) potential energy matrix for the 1^- state of ${}^7\text{Li}$. Results are obtained with the MHNP.

these nuclei. This means that the total orbital momentum $L = 0$ for even nuclei (${}^6\text{Li}$ and ${}^8\text{Be}$) and $L = 1$ for odd nuclei (${}^5\text{He}$, ${}^5\text{Li}$, ${}^7\text{Li}$ and ${}^7\text{Be}$).

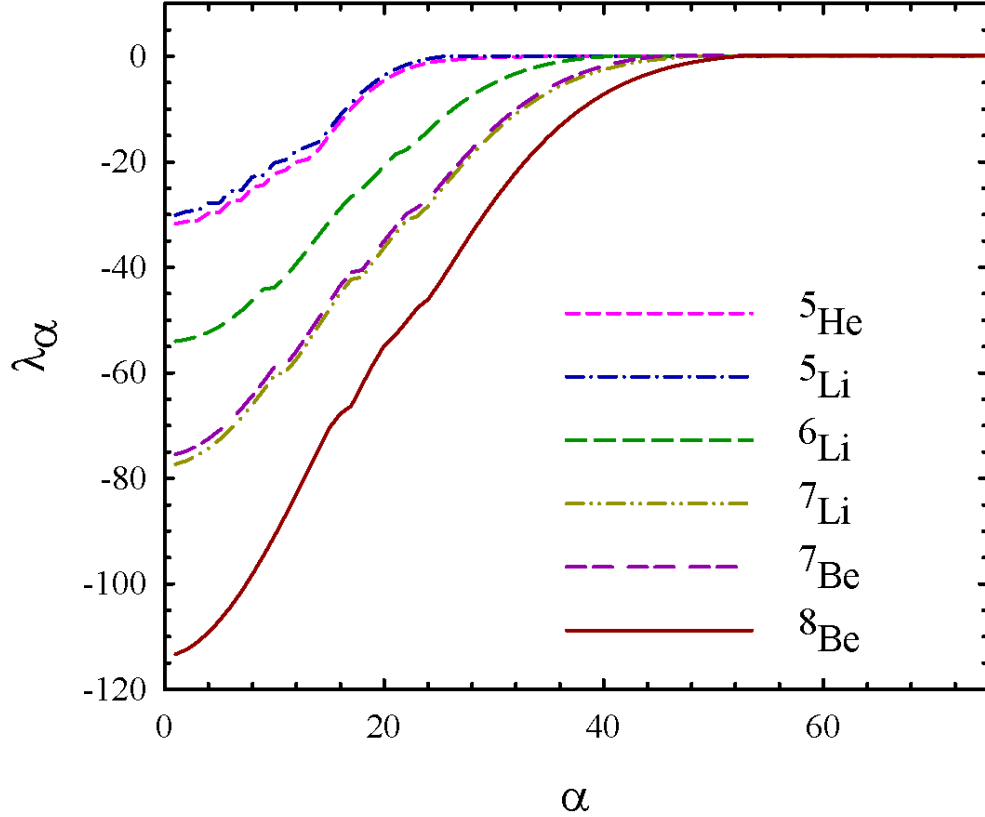


Figure 9: Eigenvalues of the potential energy matrix for the ground state of p -shell nuclei. Results are obtained with the MHNP.

One can see that the heavier is a nucleus, the deeper is the effective potential. One also notices, by comparing results for ${}^5\text{He}$ and ${}^5\text{Li}$, ${}^7\text{Li}$ and ${}^7\text{Be}$, that the Coulomb interaction slightly modifies the eigenvalues λ_α for moderate values of $\alpha < 50$. However, the strongest effect we observe for maximal values of α . Indeed, in Fig. 10 we display λ_α which are positive. We assume that these eigenvalues for nuclei ${}^6\text{Li}$, ${}^7\text{Li}$, ${}^7\text{Be}$ and ${}^8\text{Be}$ are originated from the Coulomb interaction. It will be proved later by comparing the eigenvalues of the exact and folding potential energy operators. Here, we

point out that the eigenvalues of the potential energy of nuclei having the same total charge Z and cluster charges Z_1 and Z_2 are very close to each other. Indeed, the lines representing nuclei ${}^5\text{Li}$, ${}^6\text{Li}$ and ${}^7\text{Li}$ lie very close. The same is true for the nuclei ${}^7\text{Be}$ and ${}^8\text{Be}$.

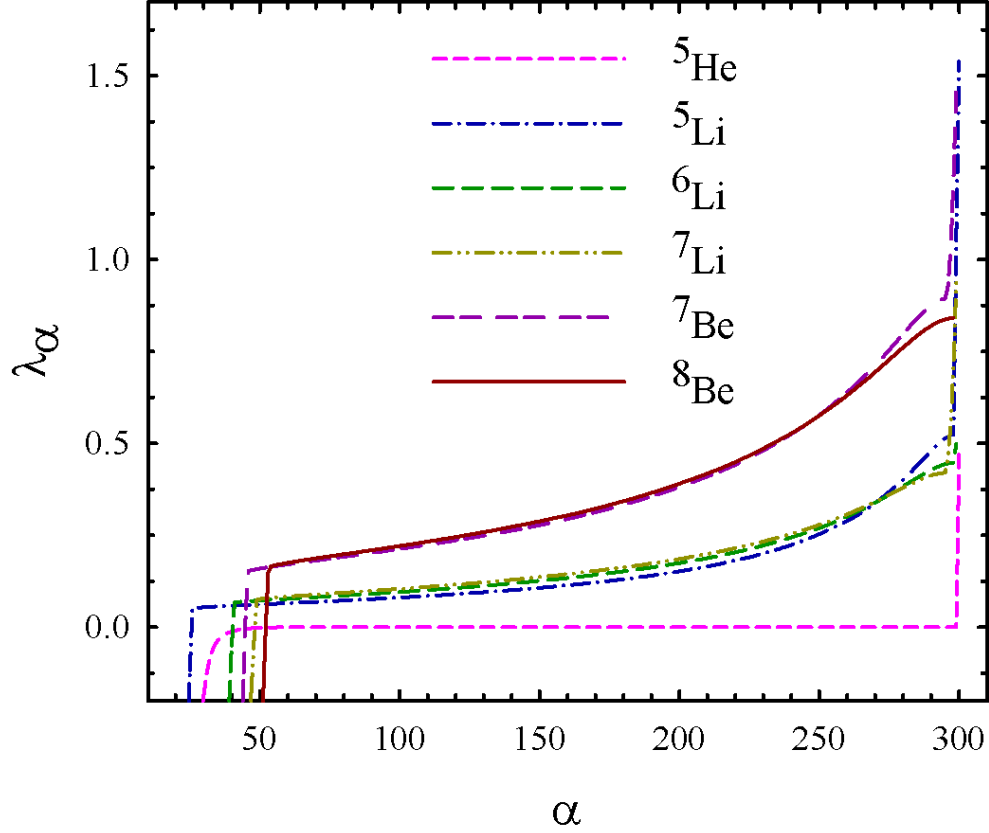


Figure 10: The eigenvalues λ_α for large values of α generated by the MHNP.

As we can see in Fig. 10, for large values of α , the exact eigenvalues λ_α are very close to the folding eigenvalues. However, in the vicinity of the final value of $\alpha = 300$, we observe a noticeable difference of eigenvalues λ_α . Thus we need a closer look at the structure of these unusual eigenstates, for which the abbreviation HES (highly-excited eigenstate) is used.

Having analyzed eigenvalues of all nuclei, we came to the conclusion that

HES are observed for the normal parity states of all nuclei but ^8Be . For the abnormal parity states we found out the HES only in ^5He and ^5Li . The number of the HES depends on the nucleus and is independent on the nucleon-nucleon potential. For ^5He , ^5Li , ^6Li , there is only one HES, and for ^7Li and ^7Be the number of such states equals 4. In Fig. 11 we demonstrate the eigenvalues λ_α with $\alpha \geq 50$. This figure shows the eigenvalues λ_α for the 1^- and 3^- states in ^7Li , obtained with and without antisymmetrization. In the neighborhood of a point $\alpha=300$ the four HES appear in the 1^- and 3^- states. The eigenvalues λ_α of these state slightly depend on the total orbital momentum L .

Detailed analysis of wave functions of the HES will be presented at the end of this section.

Fig. 12 demonstrates how the eigenvalues of the potential energy operator depend on the total orbital momentum. In Fig. 12 we display the eigenvalues for ^8Be obtained with the MHNP. We see that the eigenvalues of the exact potential energy operator slightly depend on the total orbital momentum. A similar picture is observed for other nuclei and for other nucleon-nucleon potentials.

In Fig. 13 we show dependence of the eigenvalues λ_α on the number N of oscillator functions involved in calculations. These results are obtained for $L^\pi = 1^-$ state of ^7Li with the MHNP.

One can see that the more functions involved, the more dense is the spectrum of eigenstates. One also notices three plateaus created by the eigenstates which can be treated as "resonance" states. It is because such plateau in the dependence of the eigenvalues of a Hamiltonian indicate that a system under consideration has resonance states. They are called the Harris eigenstates [45, 46]. The energy of such plateau is used to locate the position of a narrow resonance state in the stabilization method [47]. We will discuss properties of such states in the next subsection.

Fig. 14, where the eigenvalues of the 0^+ state in ^6Li are shown, demonstrates another interesting feature of the eigenvalues of potential energy operator generated by the Volkov NN potential: appearance of bound or trapped states. As we can see, the first eigenvalue λ_1 is almost independent on the number of oscillator functions when $N \geq 5$. For a two-cluster Hamiltonian, such a behavior of eigenvalues indicates that there is a deeply bound state with a compact two-cluster configuration. That is why we called the first eigenvalue λ_1 of the potential energy matrix a bound or trapped state. Such a behavior of eigenstates is observed also for the $L^\pi = 1^-$ states in ^5He and

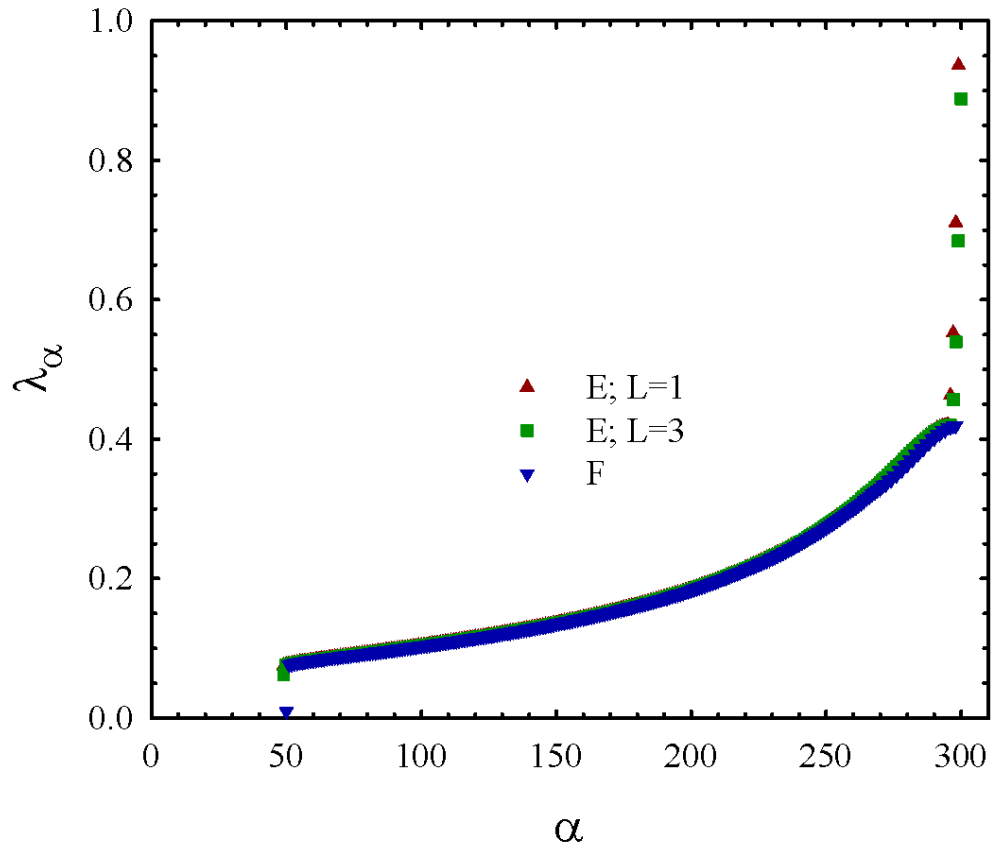


Figure 11: The largest eigenvalues generated by the MHNP for the 1^- and 3^- states in ${}^7\text{Li}$.

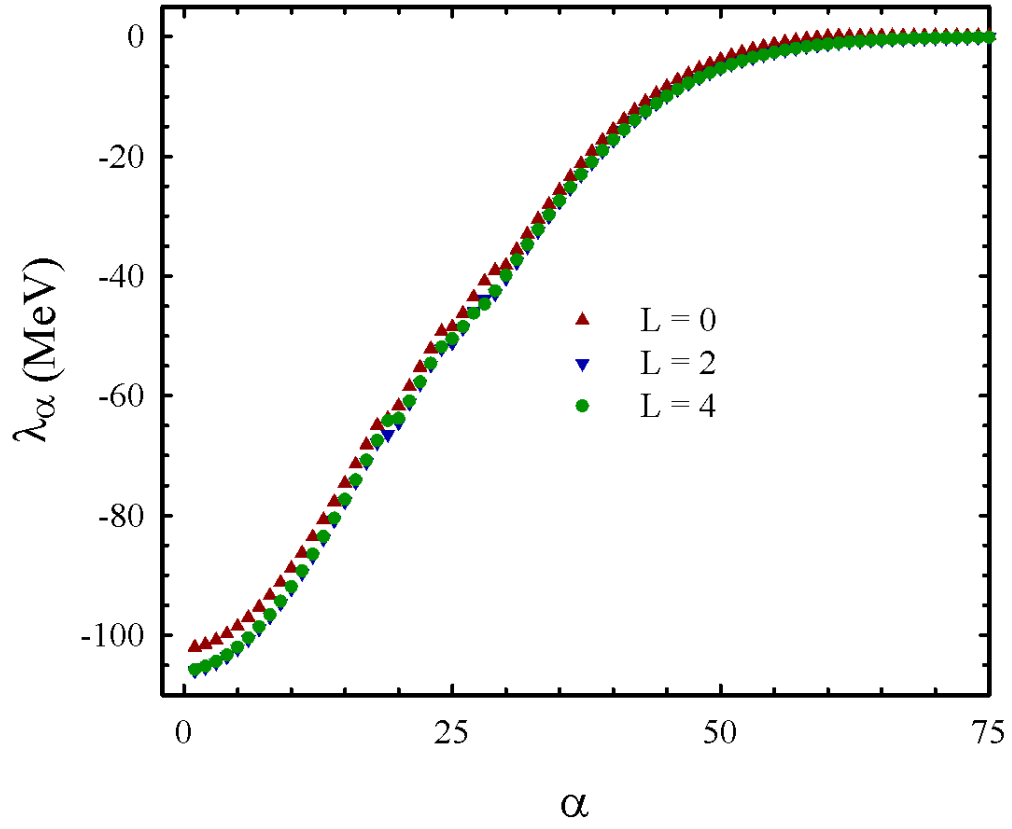


Figure 12: The eigenvalues of matrixes of potential energy operator generated by the MHNP potential for ${}^8\text{Be}$ with the total angular momentum $L=0, 2$ and 4 .

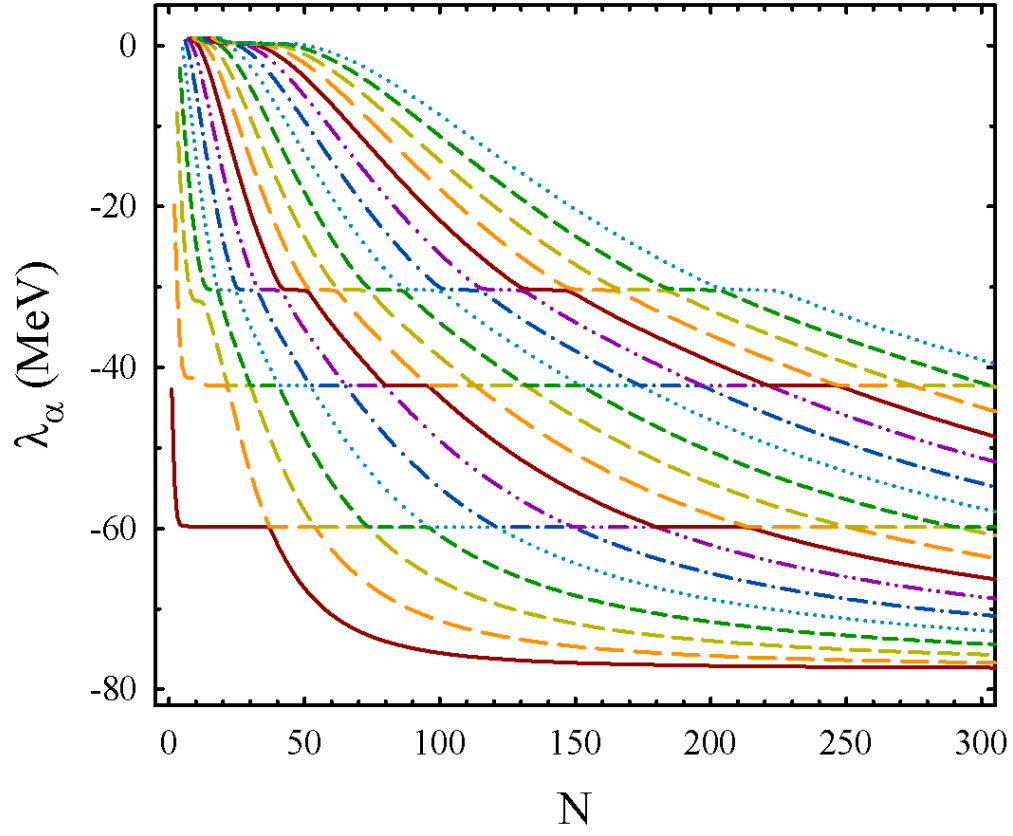


Figure 13: Eigenvalues of the potential energy matrix as a function of the number N of oscillator functions involved in calculations. Results are obtained for the 1^- state in ${}^7\text{Li}$ with the MHNP.

${}^5\text{Li}$ with the MP and VP potentials, for the $L^\pi = 0^+$ states in ${}^6\text{Li}$ with the MP and VP and for the $L^\pi = 2^+$ with the VP. In ${}^7\text{Li}$ and ${}^7\text{Be}$ such a state is found for the 1^- state with the VP only.

3.4. Eigenfunctions

Consider eigenvectors of the potential energy matrix for the 0^+ state in ${}^8\text{Be}$ and for the 1^- state in ${}^7\text{Li}$. In Fig. 15 we compare eigenvectors for ${}^8\text{Be}$ with and without antisymmetrization for the MHNP. One can see that they are quite different. The Pauli principle makes zero the first 50 expansion coefficients U_n^α .

In Fig. 16 we observe the same behavior of the eigenfunctions for the 1^- state in ${}^7\text{Li}$.

Eigenfunctions of ${}^8\text{Be}$ obtained with different NN potentials are displayed in Fig. 17. We demonstrate the eigenfunctions in the momentum space for $\alpha = 1, 2$ and 3 . A huge repulsive core in the MHNP and the Pauli principle make eigenfunctions $\phi_\alpha(p)$ to vanish in a large range of $0 < p < 10 \text{ fm}^{-1}$, while a rather modest core in the MP reduces this region to $p \approx 6 \text{ fm}^{-1}$. The eigenfunctions $\phi_\alpha(p)$ obtained with the VP exhibit only effects of the Pauli principle, since this potential has a negligibly small repulsive core.

Behavior of the eigenfunctions $\phi_\alpha(p)$ in the momentum space is compatible with the behavior of these eigenfunctions U_n^α in the oscillator space. Indeed, in Fig. 18 we observe the same impact of the Pauli principle and a core of the NN potentials on the eigenfunctions U_n^α .

By comparing eigenvalues and eigenfunctions of the mirror nuclei ${}^5\text{He}$ and ${}^5\text{Li}$, ${}^7\text{Li}$ and ${}^7\text{Be}$, we came to the conclusion that the Coulomb forces have a small impact on the matrix of the potential energy operator and its eigenvalues and eigenfunctions. We do not compare the eigenfunctions of the mirror nuclei as they are almost undistinguished.

3.4.1. Resonance and trapped states wave functions.

Now we consider wave functions of bound (trapped) and resonance states in the two-cluster systems. We start with the wave functions of a trapped 0^+ state in ${}^6\text{Li}$. They are displayed in the momentum space in Fig. 19. One can see that these functions describe a compact configuration and slightly depend on the shape of the nucleon-nucleon potentials. Besides, the wave functions obtained with the MP and VP have an exponential asymptotic behavior (Fig. 20). Thus, there is a full resemblance of these functions with a true bound state wave function which is usually observed in coordinate space. As for the

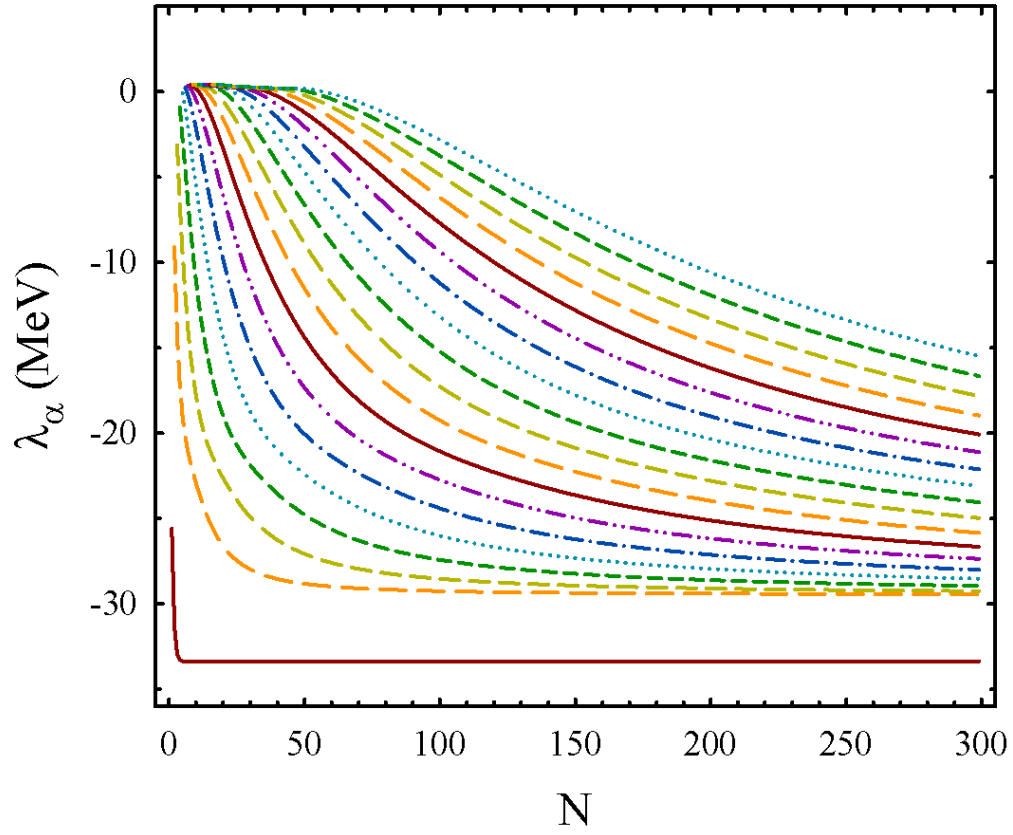


Figure 14: Dependence of eigenvalues of the 0^+ state in ${}^6\text{Li}$ on the number of oscillator functions involved in calculations. Results are obtained with the VP.

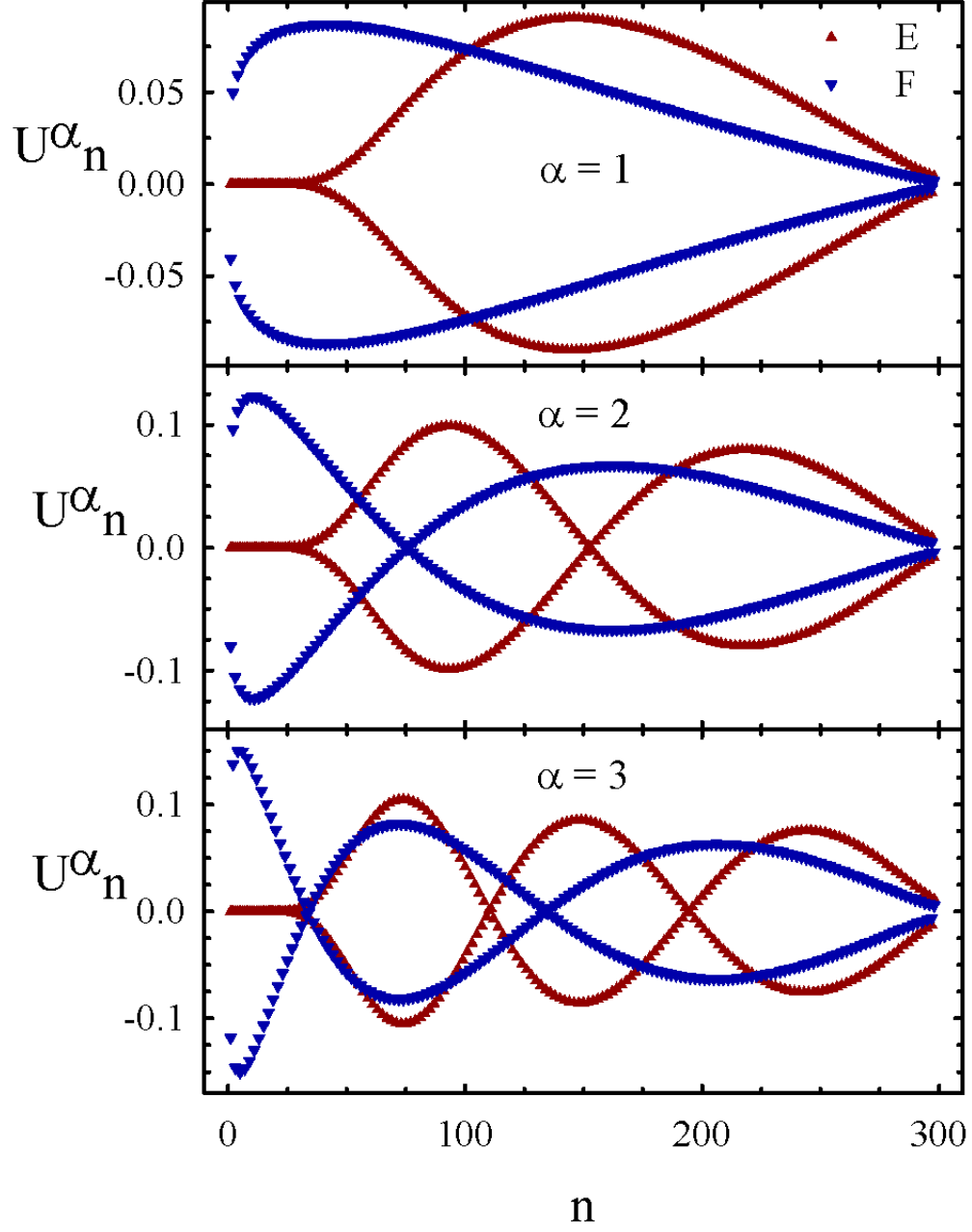


Figure 15: The eigenfunctions of the exact (E) and folding (F) potential energy in oscillator representation for the 0^+ state in ^8Be . Results are obtained with the MHNP.

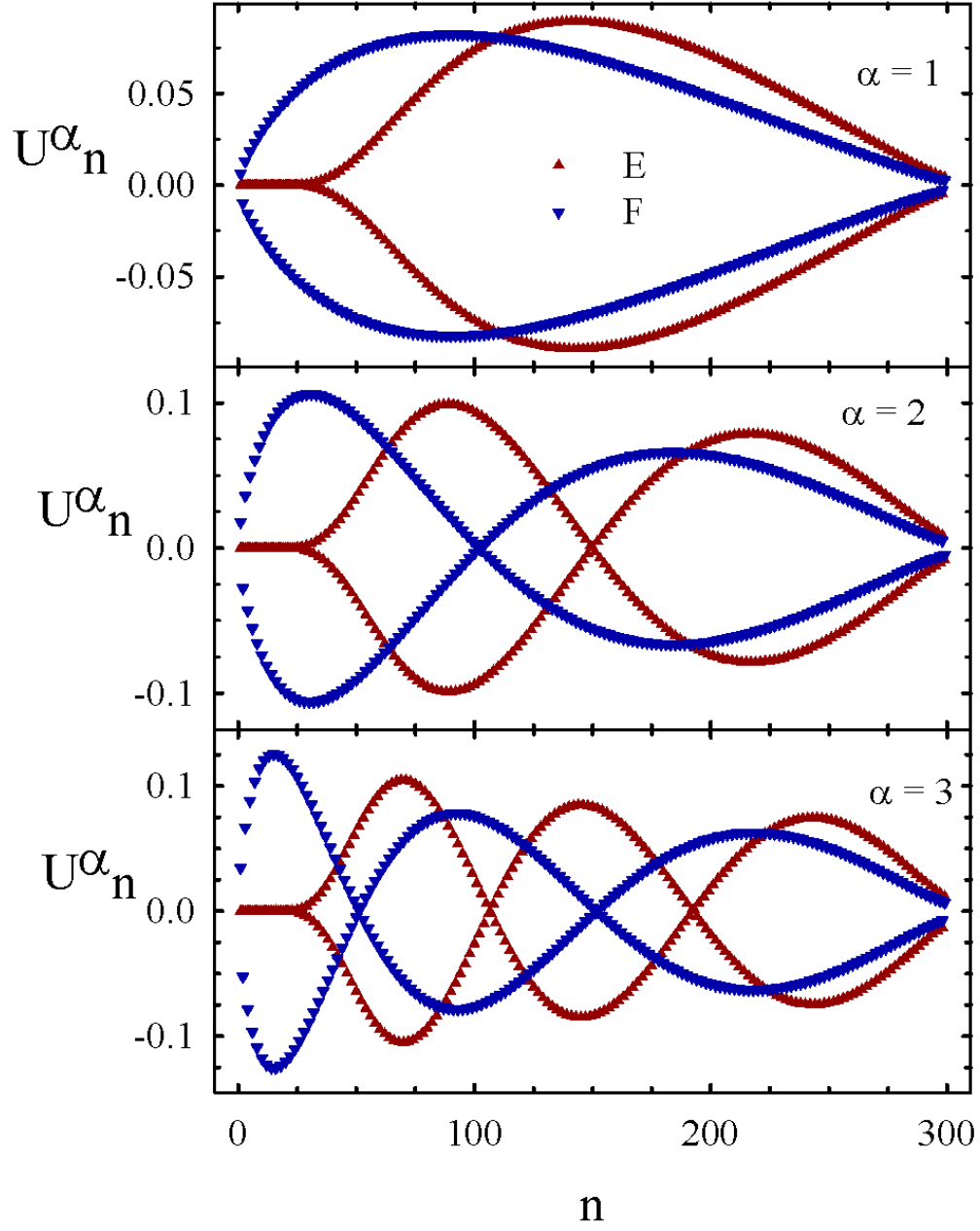


Figure 16: The eigenfunctions of the potential energy matrix generated by the MHNP for the 1^- state in ${}^7\text{Li}$.

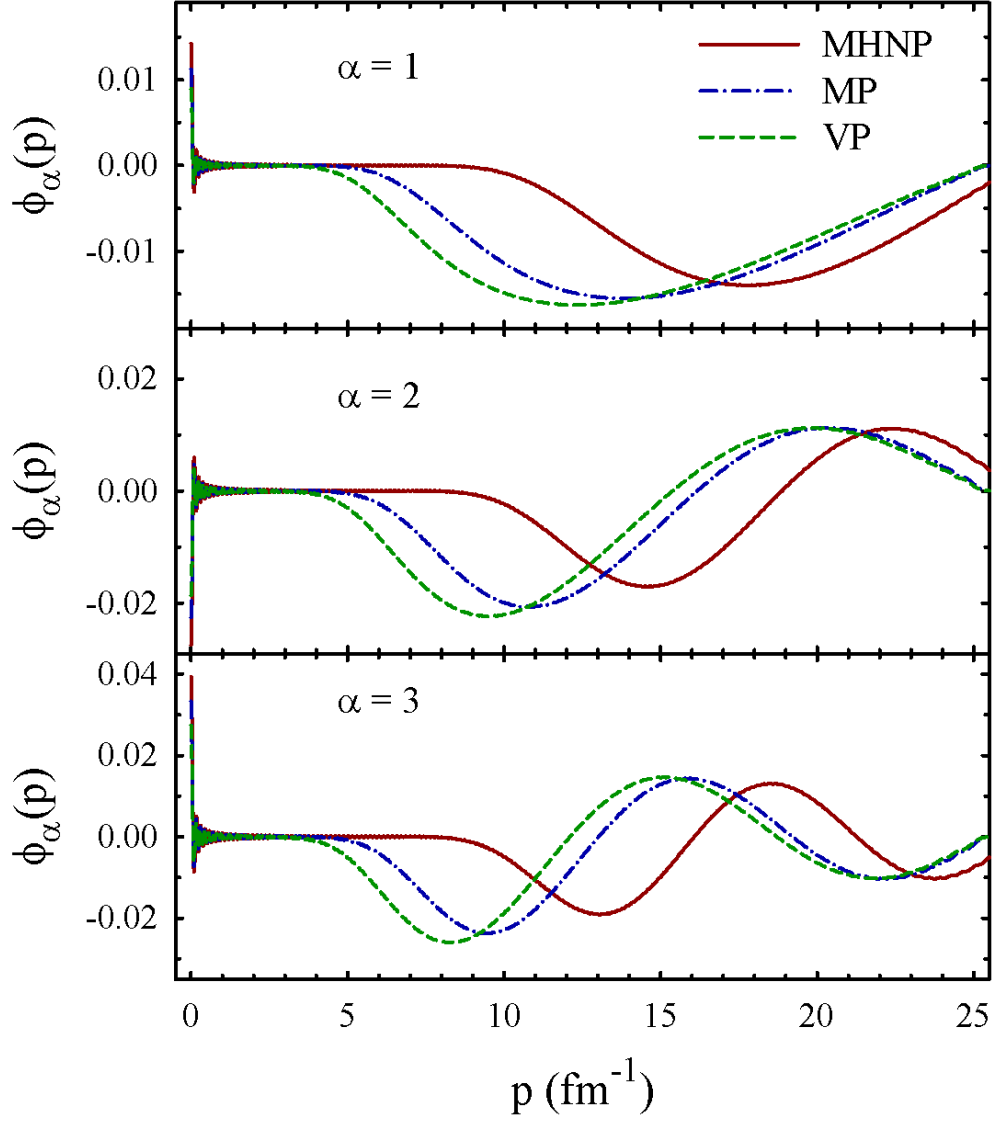


Figure 17: Eigenfunctions of the potential energy matrix obtained for the 0^+ state in ${}^8\text{Be}$ with different NN potentials.

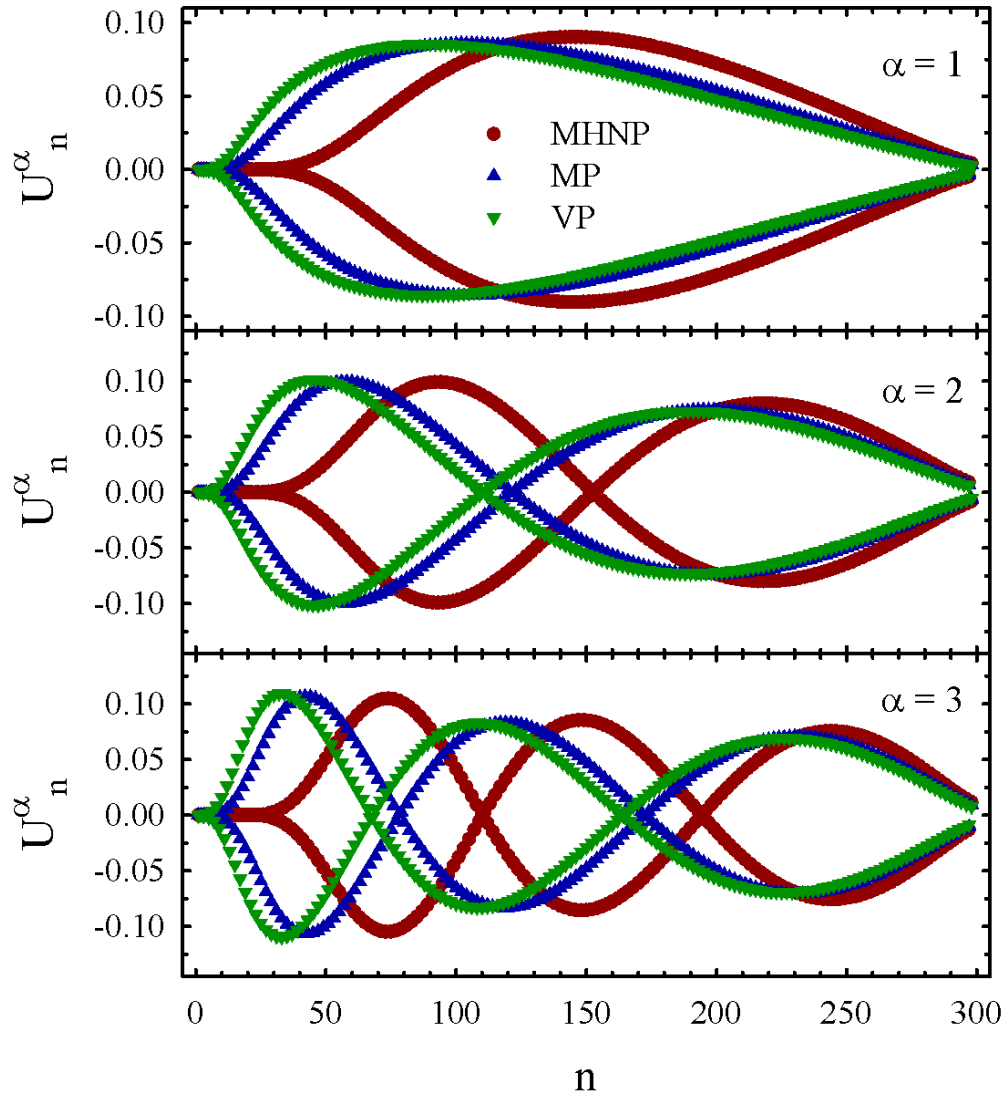


Figure 18: The eigenfunctions of the potential energy operator for the 0^+ state in ^8Be in the oscillator representation.

MHNP, the asymptotic part of the wave function has an oscillatory behavior (Fig. 20) which is typical for wave functions of a narrow resonance state. It is important to note that for the VP and MP we have got the trapped state for this nucleus, they are the lowest eigenstates ($\alpha=1$) for these potentials. It can be seen from Fig. 20 that the VP creates deeper trapped state than the MP, as the wave function obtained with VP is decreased faster than the wave function generated by the MP. The resonance state obtained with the MHNP is the $\alpha=10$ th eigenstate. An interesting feature of the wave functions presented in Fig. 19 that they have a node at $p \approx 1.0 \text{ fm}^{-1}$. Such a behavior of eigenfunctions of the trapped state is similar to the behavior of the wave function in coordinate representation of the ground state of ${}^6\text{Li}$, obtained within a two-cluster model (see Fig. 5 in Ref. [48]). The node of the bound state wave functions appears due to the orthogonality of this state to the Pauli forbidden state(s) in two-cluster systems.

The trapped and resonance states are compact states, because their wave functions dominates at small values of coordinate (q), momentum (p) and oscillator (n) spaces.

Wave functions $\phi_\alpha(p)$ of the first $L^\pi = 1^-$ resonance eigenstate in ${}^7\text{Li}$ generated by different NN potentials are displayed in Fig. 21. This figure demonstrates that the shape of these functions slightly depends on the peculiarities of the nucleon-nucleon potential. The wave functions $\phi_\alpha(p)$ equal zero at $p = 0$, as these functions describe the relative motion of clusters with the orbital momentum $L = 1$.

Let us have a closer look at the wave functions of the highly-excited eigenstates. In Fig. 22 we demonstrate the eigenfunctions $\phi_\alpha(p)$ of such states in the momentum representation. These functions are determined for the 1^- state in ${}^7\text{Li}$ with the MHNP. This is the most exotic case with four highly-excited eigenfunctions. As we see, these functions describe a compact two-cluster configuration. They are similar to the resonance wave functions. The compactness of the HES is also observed in the oscillator and coordinate representations. An asymptotic part of the eigenfunctions $\phi_\alpha(p)$ exhibits an oscillatory behavior with the amplitude which is much smaller than the amplitude in the internal region. The eigenfunction for $\alpha = 300$ with the largest value of λ_α corresponds to the most compact two-cluster configuration. The smaller is the eigenvalue λ_α , the less compact is the two-cluster system. Or, in other words, the smaller is the eigenvalue λ_α , the smaller is the width of such resonance state.

By comparing Figs. 21 and 22, we see a certain similarity of the low-

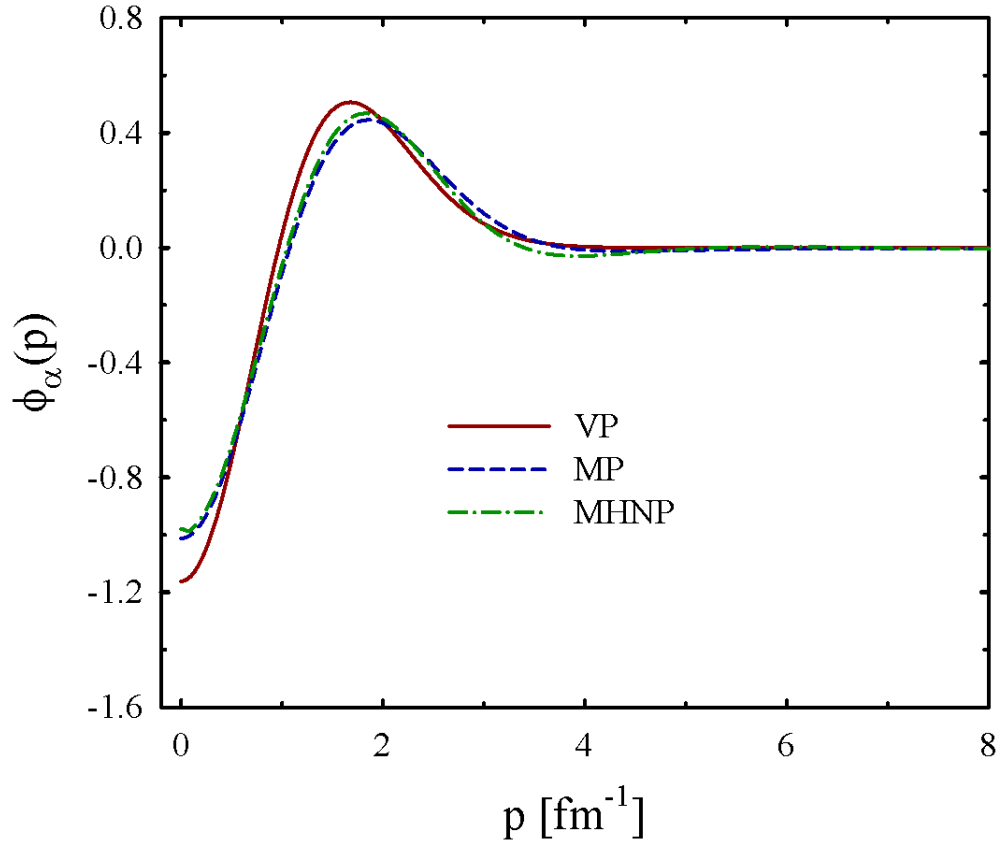


Figure 19: Wave functions of the trapped and resonance 0^+ states in ${}^6\text{Li}$ as a function of momentum p .

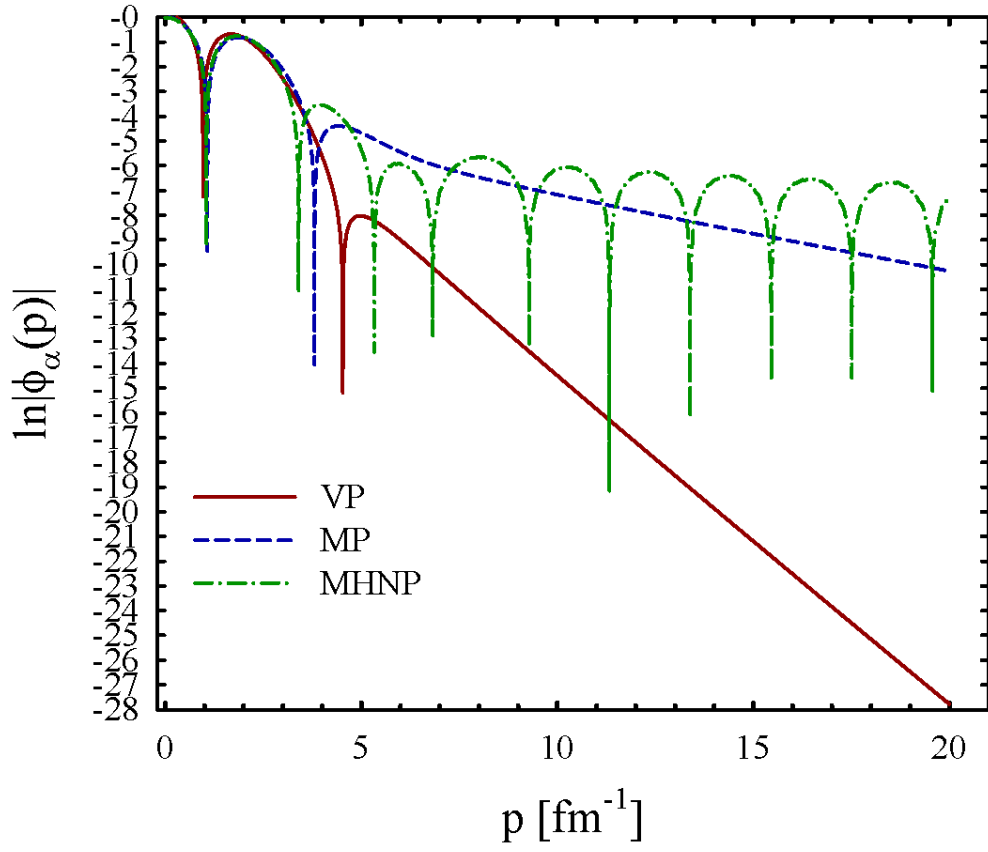


Figure 20: Asymptotic behavior of the wave functions of the 0^+ state in ${}^6\text{Li}$.

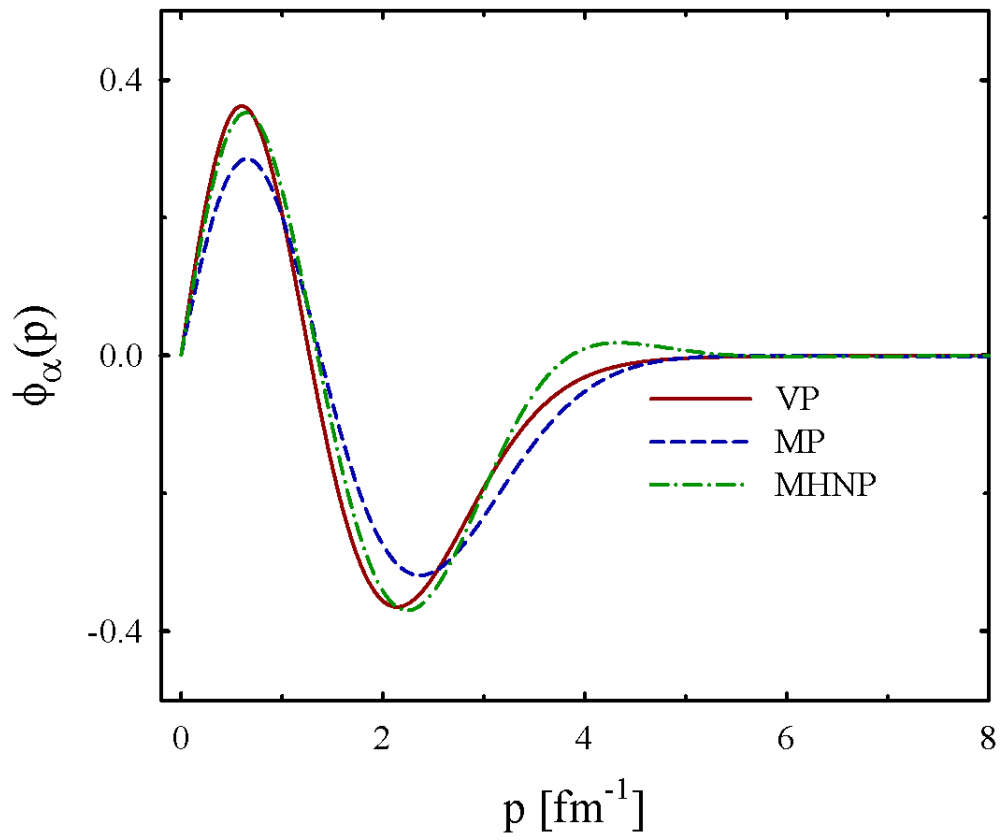


Figure 21: Wave functions of the first $L^\pi = 1^-$ resonance eigenstate in ${}^7\text{Li}$.

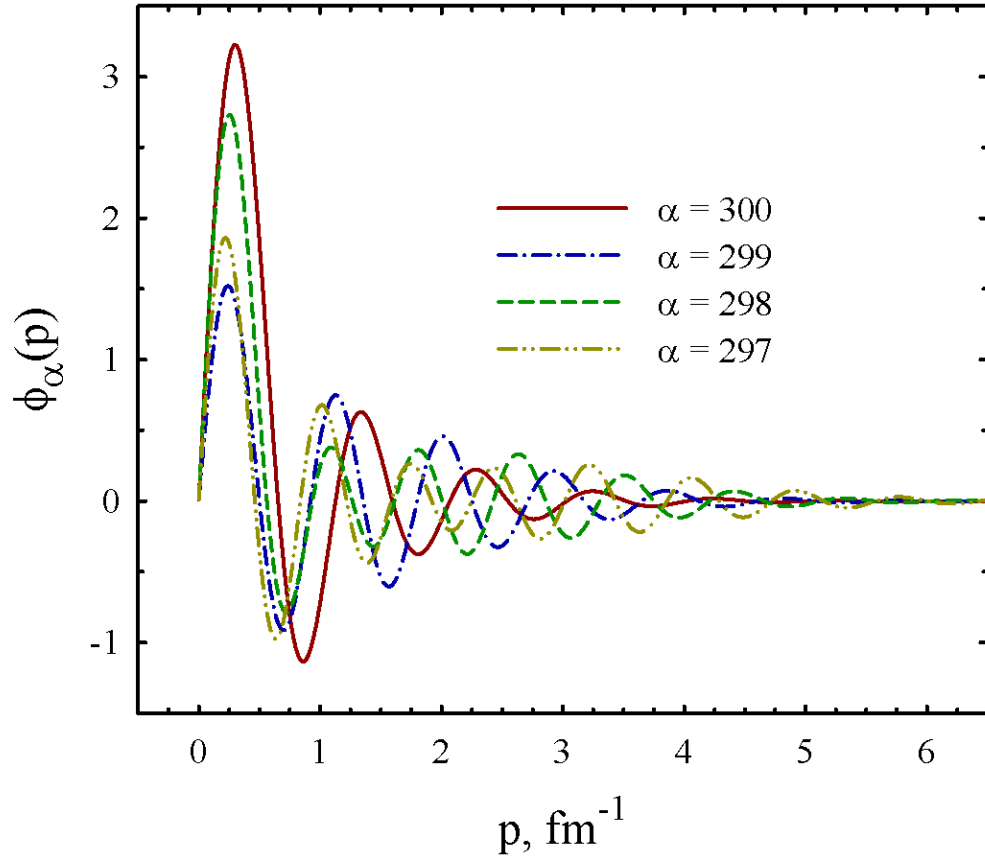


Figure 22: The eigenfunctions $\phi_\alpha(p)$ of the potential energy matrix corresponding to the highly-excited eigenstates. These functions are obtained for the 1^- state in ${}^7\text{Li}$ with MHNP.

energy and highly-excited resonance states. The wave functions of both states have large amplitude at small values of the momentum p . The main difference between these states is that the wave functions of the highly-excited states have more nodes as they correspond to higher energy than the low-energy resonance states.

If we consider the evolution of the highly excited eigenvalues λ_α with the increasing number N of the invoked basis functions, we observe the stability of the corresponding eigenvalues λ_α , which is similar to the stability of bound and resonance states displayed in Figs 13, 14. As we can see in Fig. 23, the last four eigenstates λ_α are stable when $N \geq 25$.

3.5. Interpretation of eigenfunctions

The shape of the eigenfunctions in the momentum representation suggests that they are wave functions of a particle in a field of a step potential. The range of such a potential should be approximately of 7-10 fm. And the height of the step potential should be large enough to suppress the wave function inside this potential. However, appearance of "resonance states" or "trapped states" somewhat contradicts this suggestion. It is known, see, for example, book [49], that the step potential creates resonance states with the energy which is larger than the height of the potential. The step potential cannot create a very narrow resonance states. Besides, the nodes of wave functions of the trapped or resonance states has to be taken into account. To establish the explicit form of the auxiliary Hamiltonian \hat{H}_a

$$\hat{H}_a = \hat{T}_p + \hat{V}_a(p), \quad (26)$$

which possess the following property

$$\hat{H}_a \phi_\alpha(p) = \mathcal{E}_\alpha \phi_\alpha(p),$$

one needs to perform a large number of numerical experiments. Thus this problem will be considered elsewhere.

4. Conclusions

We have investigated effects of antisymmetrization on the potential energy of two clusters interaction. For this aim we have studied eigenfunctions and eigenvalues of the potential energy matrix, calculated within a basis of

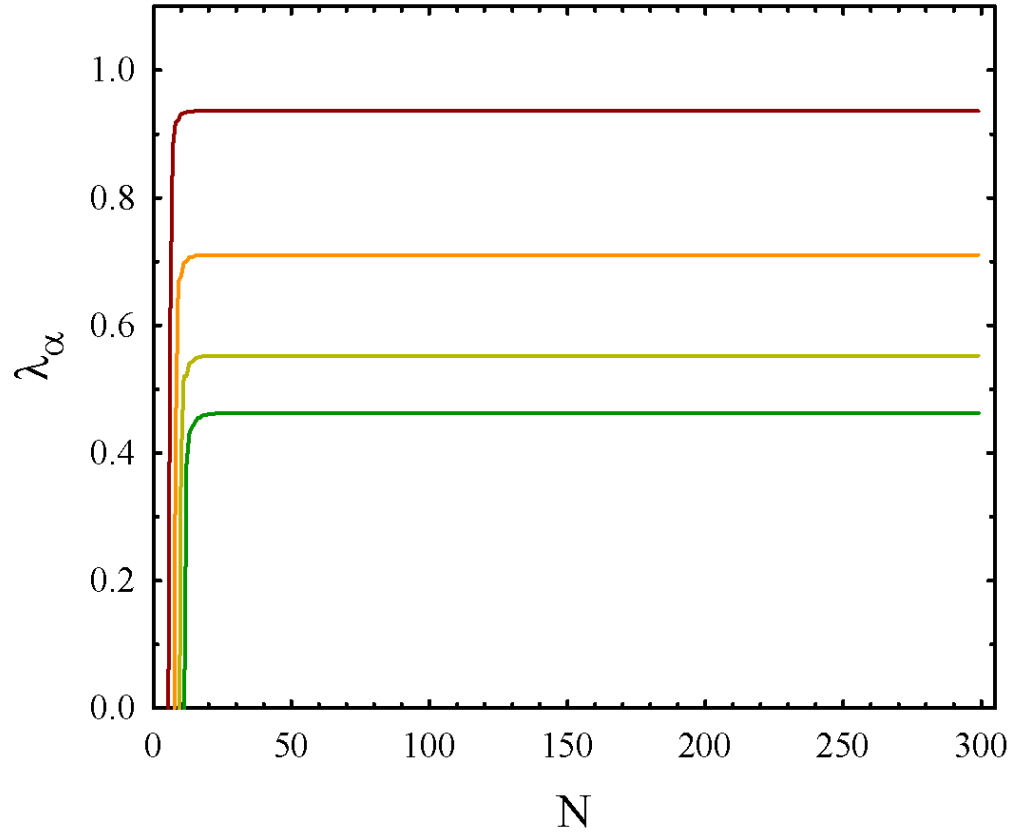


Figure 23: The dependence of the eigenvalues λ_α belonging to the highly-excited states on the number of oscillator functions involved in calculations. Results are presented for the 1^- state in ${}^7\text{Li}$ and the MHNP.

the cluster oscillator functions. It was shown that eigenvalues of the potential energy calculated with the full antisymmetrization are close to the ones, obtained in the folding approximation. However, the eigenfunctions in those cases are quite different. In the folding model the eigenfunctions are the free-motion Bessel functions, while the antisymmetrization generates functions which are similar to the functions, describing scattering states on a step potential. However, to establish the exact nature of these eigenfunctions one needs to perform enhanced investigations. This is planned to do in the next publication.

By analyzing the evolution of the eigenvalues of the potential energy operator with increasing the number N of oscillator functions, we have discovered the trapped and resonance states. The trapped states represent themselves as a state with a stable and almost independent on N the lowest eigenvalue λ_1 . The resonance states exhibit themselves as a plateau in the dependence of the eigenvalues λ_α on the number N of the basis functions involved in the calculations. Both trapped and resonance states have a compact wave function of two-cluster systems. This compactness is observed in the oscillator, momentum and coordinate spaces. The trapped states have an exponential asymptotic tail, while the resonance states have an oscillating asymptotic tail.

We have also discovered the highly-excited resonance states. They have the largest eigenvalues and mainly exhibit themselves in the normal parity states in all nuclei but ^8Be . The largest number (four) of the highly-excited resonance states are observed in ^7Li and ^7Be and only one state is found in other nuclei. The highly-excited states describe a compact two-cluster structure which can be seen in the oscillator, coordinate and momentum representations.

By closing the present paper we would like to indicate the further steps of development of the suggested method and obtained results.

First, the obtained eigenfunctions and eigenvalues of the matrix of potential energy operator can be used to construct the wave functions and t-matrix for two-cluster systems in a similar way as it was done in Ref. [33] for two-body potentials. This may suggest an alternative form of the dynamic equations to that which is now used within the algebraic version of the resonating group method. This is definitely a subject for a separate paper.

Second, it is also interesting to study properties of the potential energy operator for three-cluster system when a several two-cluster channels and a large number of three-cluster channels are open. This will be studied in other

papers.

5. Acknowledgment

The present work was partially supported by the Program of Fundamental Research of the Department of Physics and Astronomy of the National Academy of Sciences of Ukraine (project No. 0117U000239).

References

- [1] G. F. Filippov, I. P. Okhrimenko, Use of an oscillator basis for solving continuum problems, *Sov. J. Nucl. Phys.* **32** (1981) 480–484.
- [2] G. F. Filippov, On taking into account correct asymptotic behavior in oscillator-basis expansions, *Sov. J. Nucl. Phys.* **33** (1981) 488–489.
- [3] J. A. Wheeler, Molecular Viewpoints in Nuclear Structure, *Phys. Rev.* **52** (1937) 1083–1106. doi:10.1103/PhysRev.52.1083.
- [4] J. A. Wheeler, On the Mathematical Description of Light Nuclei by the Method of Resonating Group Structure, *Phys. Rev.* **52** (1937) 1107–1122. doi:10.1103/PhysRev.52.1107.
- [5] S. Saito, Theory of Resonating Group Method and Generator Coordinate Method, and Orthogonality Condition Model, *Prog. Theor. Phys. Suppl.* **62** (1977) 11–89. doi:10.1143/PTPS.62.11.
- [6] Y. C. Tang, M. Lemere, D. R. Thompson, Resonating-group method for nuclear many-body problems, *Phys. Rep.* **47** (1978) 167–223. doi:10.1016/0370-1573(78)90175-8.
- [7] Y. C. Tang, Microscopic description of the nuclear cluster theory, in: T. S. Kuo, S. M. Wong (Eds.), *Topics in Nuclear Physics II A Comprehensive Review of Recent Developments*, Vol. 145 of *Lecture Notes in Physics*, Berlin Springer Verlag, 1981, pp. 571–692. doi:10.1007/BFb0017230.
- [8] K. Wildermuth, Y. Tang, *A unified theory of the nucleus*, Vieweg Verlag, Braunschweig, 1977.

- [9] I. V. Kurdyumov, Y. F. Smirnov, K. V. Shitikova, S. K. E. Samarai, Translationally invariant shell model, Nucl. Phys. A 145 (1970) 593–612. doi:10.1016/0375-9474(70)90444-6.
- [10] V. G. Neudachin, Yu. F. Smirnov, Nucleon associations in light nuclei (in Russian), 'Nauka', Moscow, 1969.
- [11] J. Revai, A new method of calculating wave functions on harmonic oscillator basis, Preprint JINR, Dubna, E4-9429 (1975) 12 pp.
- [12] L. Majling, J. Rizek, Z. Pluhar, Y. F. Smirnov, On some peculiarities of the variational calculations in the harmonic oscillator basis, J. Phys. G: Nucl. Phys. **2** (1976) 357–364.
- [13] M. Moshinsky, The Harmonic oscillator in Modern Physics: From Atoms to Quarks, Gordon Breach, New-York, London, Paris, 1969.
- [14] D. Baye, P.-H. Heenen, M. Libert-Heinemann, Microscopic R-matrix theory in a generator coordinate basis (III). Multi-channel scattering, Nucl. Phys. A 291 (1977) 230–240. doi:10.1016/0375-9474(77)90208-1.
- [15] S. Quaglioni, P. Navrátil, Ab initio many-body calculations of nucleon-nucleus scattering, Phys. Rev. C 79 (4) (2009) 044606. arXiv:0901.0950, doi:10.1103/PhysRevC.79.044606.
- [16] S. Quaglioni, C. Romero-Redondo, P. Navrátil, Three-cluster dynamics within an ab initio framework, Phys. Rev. C 88 (3) (2013) 034320. arXiv:1307.8160, doi:10.1103/PhysRevC.88.034320.
- [17] S. Saito, Interaction between Clusters and Pauli Principle, Prog. Theor. Phys. **41** (3) (1969) 705–722. doi:10.1143/PTP.41.705.
- [18] V. I. Kukulin, V. G. Neudachin, V. N. Pomerantsev, Exclusion of Occupied States in the Faddeev Equations for Three Composite Particles, Yad. Fiz. 24 (1976) 298–307.
- [19] V. I. Kukulin, V. N. Pomerantsev, Rearrangement and improvement of convergence of the born series in scattering theory on the basis of orthogonal projections, Theor. Math. Phys. 27 (1976) 549–557. doi:10.1007/BF01028623.

- [20] V. I. Kukulin, V. N. Pomerantsev, The orthogonal projection method in scattering theory, *Ann. Phys.* 111 (1978) 330–363. doi:10.1016/0003-4916(78)90069-6.
- [21] Y. Fujiwara, H. Horiuchi, Generator Coordinate Theory of Normalization Kernels of Cluster Systems. I, *Prog. Theor. Phys.* 63 (1980) 895–918.
- [22] H. Horiuchi, Multi-Cluster Allowed States and Spectroscopic Amplitude of Cluster Transfer, *Prog. Theor. Phys.* 58 (1977) 204–222.
- [23] Y. Fujiwara, H. Horiuchi, Generator Coordinate Theory of Normalization Kernels of Cluster Systems. II —Systems Described by Three Generator Coordinate Vectors Involving Complex Conjugate One(s)—, *Prog. Theor. Phys.* 65 (1981) 1632–1666.
- [24] Y. Fujiwara, H. Horiuchi, Generator Coordinate Theory of Normalization Kernels of Cluster Systems. III —Application of Double Gel’fand Polynomials to General Cluster Systems—, *Prog. Theor. Phys.* 65 (1981) 1901–1927.
- [25] Y. Fujiwara, Y. C. Tang, H. Horiuchi, Generator Coordinate Theory of Normalization Kernels of Cluster Systems. IV —Application of Double Gel’fand Polynomials to SU_4 Symmetry of Cluster Wave Functions—, *Prog. Theor. Phys.* 70 (1983) 809–826. doi:10.1143/PTP.70.809.
- [26] H. Horiuchi, K. Yabana, Pauli-Forbidden Region in the Phase-Space of Coupled-Channel System in the Framework of the Time-Dependent Variational Theory, *Prog. Theor. Phys.* 72 (1984) 1277–1281.
- [27] K. Kato, K. Fukatsu, H. Tanaka, Systematic Construction Method of Multi-Cluster Pauli-Allowed States, *Prog. Theor. Phys.* 80 (4) (1988) 663–677. doi:10.1143/PTP.80.663.
- [28] G. F. Filippov, Y. A. Lashko, S. V. Korennov, K. Katō, Norm Kernels and the Closeness Relation for Pauli-Allowed Basis Functions, *Few-Body Syst.* 33 (2003) 173–198. doi:10.1007/s00601-003-0009-z.
- [29] G. Filippov, Y. Lashko, Peculiar properties of the cluster-cluster interaction induced by the Pauli exclusion principle, *Phys. Rev. C* 70 (6) (2004) 064001. doi:10.1103/PhysRevC.70.064001.

- [30] G. Filippov, Y. Lashko, Structure of Light Neutron-Rich Nuclei and Nuclear Reactions Involving These Nuclei, *El. Chast. Atom. Yadra* **36** (6) (2005) 1373–1424.
- [31] Y. A. Lashko, G. F. Filippov, The role of the Pauli principle in three-cluster systems composed of identical clusters, *Nucl. Phys. A* **826** (2009) 24–48. [arXiv:0811.1695](#), [doi:10.1016/j.nuclphysa.2009.05.071](#).
- [32] Y. A. Lashko, G. F. Filippov, How the Pauli principle governs the decay of three-cluster systems, *Nucl. Phys. A* **806** (2008) 124–145. [arXiv:0712.4013](#), [doi:10.1016/j.nuclphysa.2008.03.003](#).
- [33] Y. A. Lashko, V. Vasilevsky, G. Filippov, Properties of a potential energy matrix in oscillator basis, *Ann. Phys.* **409** (2019) 167930. [doi:https://doi.org/10.1016/j.aop.2019.167930](#).
- [34] G. Filippov, Y. Lashko, Structure of Light Neutron-Rich Nuclei and Nuclear Reactions Involving These Nuclei, *Phys. Part. Nucl.* **36** (6) (2005) 714–739.
- [35] G. F. Filippov, V. S. Vasilevsky, L. L. Chopovsky, Solution of problems in the microscopic theory of the nucleus using the technique of generalized coherent states, *Sov. J. Part. Nucl.* **16** (1985) 153–177.
- [36] G. F. Filippov, V. S. Vasilevsky, L. L. Chopovsky, Generalized coherent states in nuclear-physics problems, *Sov. J. Part. Nucl.* **15** (1984) 600–619.
- [37] S. Saito, Effect of Pauli Principle in Scattering of Two Clusters, *Prog. Theor. Phys.* **40** (1968) 893–894. [doi:10.1143/PTP.40.893](#).
- [38] A. Zubarev, Separabilization method in the problems of nuclear physics, *El. Chast. Atom. Jadra* **7** (2) (1976) 553–583.
- [39] V. B. Belyaev, Lectures on theory of few body systems. (In Russian), *Energoatomizdat*, Moscow, 1986.
- [40] R. G. Newton, *Scattering Theory of Waves and Particles*, McGraw-Hill, New-York, 1966.

- [41] A. B. Volkov, Equilibrium deformation calculation of the ground state energies of 1p shell nuclei, Nucl. Phys. **74** (1965) 33–58. doi:10.1016/0029-5582(65)90244-0.
- [42] A. Hasegawa, S. Nagata, Ground state of ${}^6\text{Li}$, Prog. Theor. Phys. **45** (1971) 1786–1807. doi:10.1143/PTP.45.1786.
- [43] F. Tanabe, A. Tohsaki, R. Tamagaki, $\alpha\alpha$ scattering at intermediate energies, Prog. Theor. Phys. **53** (1975) 677–691.
- [44] D. R. Thompson, M. LeMere, Y. C. Tang, Systematic investigation of scattering problems with the resonating-group method, Nucl. Phys. **A286** (1) (1977) 53–66. doi:10.1016/0375-9474(77)90007-0.
- [45] F. E. Harris, Expansion Approach to Scattering, Phys. Rev. Lett. **19** (4) (1967) 173–175. doi:10.1103/PhysRevLett.19.173.
- [46] H. A. Yamani, The J-matrix reproducing kernel: Numerical weights at the Harris energy eigenvalues, J. Math. Phys. **25** (1984) 317–322. doi:10.1063/1.526152.
- [47] A. U. Hazi, H. S. Taylor, Stabilization Method of Calculating Resonance Energies: Model Problem, Phys. Rev. A **1** (1970) 1109–1120. doi:10.1103/PhysRevA.1.1109.
- [48] Y. A. Lashko, G. F. Filippov, V. S. Vasilevsky, Dynamics of two-cluster systems in phase space, Nucl. Phys. A **941** (2015) 121–144. arXiv:1503.06005, doi:10.1016/j.nuclphysa.2015.06.006.
- [49] S. Fluegge, Practical quantum mechanics, Springer, Berlin, 1971.